Chapter 18
Scattering: 3-D

In order to appreciate the intricacies of quantum-mechanical scattering, you have to know something about classical scattering. When two particles collide and undergo elastic scattering, both the classical and quantum scattering problems can be very difficult to solve. The first step in the analysis of this problem is to make a transformation to the center-of-mass frame of the two particles. Then the interaction can be reduced to the scattering of a particle having reduced mass μ from a center of potential having relative coordinate $\mathbf{r}$. One calculates the scattering in the center-of-mass frame and then must transform back to laboratory coordinates. I will discuss only the problem of scattering in the center-of-mass frame or, equivalently, scattering of a particle having mass μ from a potential $V(r)$ that is assumed to possess spherical symmetry. The particle is incident along the z axis and has energy E.

18.1 Classical Scattering

Let me first review classical scattering, indicated schematically in Fig. 18.1. The scattering depends on the *impact parameter* b and energy E of the incoming particle, as well as on the nature of $V(r)$. If the particle has initial speed $v_0 = \sqrt{2E/\mu}$, the magnitude of the particle's angular momentum, impact parameter, and energy are related by

$$|\mathbf{L}| = L = \mu v_0 b = \sqrt{2\mu E}b; \tag{18.1a}$$

$$E = \frac{L^2}{2\mu b^2}. \tag{18.1b}$$

P.R. Berman, *Introductory Quantum Mechanics*, UNITEXT for Physics,
https://doi.org/10.1007/978-3-319-68598-4_18

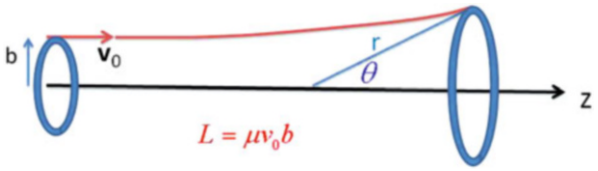

Fig. 18.1 Scattering by a spherically symmetric potential. Particles having initial velocity $\mathbf{v}_0 = v_0\mathbf{u}_z$ that are incident with an impact parameter between b and $b + db$ are scattered into a ring having area $2\pi r^2 \sin\theta d\theta$

Since the potential is spherically symmetric the angular momentum is a constant of the motion.

Moreover, as shown in Fig. 18.1, any particle incident within a ring having radius b and width db is scattered into a ring on a spherical surface having polar angle θ ($0 \leq \theta \leq \pi$), circumference $2\pi r \sin\theta$ and width $rd\theta$. Thus, the area of the ring into which the particle is scattered $d\sigma/d\Omega$ is $2\pi r^2 \sin\theta d\theta$. The *differential cross section* $d\sigma/d\Omega$ is then defined by

$$\frac{d\sigma}{d\Omega}d\Omega = \frac{\text{number of particles scattered into } d\Omega \text{ per unit time}}{I}, \tag{18.2}$$

where I is the number of particles incident per unit area per unit time and

$$d\Omega = 2\pi \sin\theta d\theta \tag{18.3}$$

is an element of solid angle. Since each particle in the ring having radius b and width db is scattered into $d\Omega$,

$$\frac{d\sigma}{d\Omega}2\pi \sin\theta d\theta = \frac{I2\pi b db}{I} \tag{18.4}$$

or

$$\frac{d\sigma}{d\Omega} = \left|\frac{b}{\sin\theta}\frac{db}{d\theta}\right| = \left|\frac{b}{\sin\theta\frac{d\theta}{db}}\right|, \tag{18.5}$$

where, by convention, $\frac{d\sigma}{d\Omega}$ is always positive. If more than one impact parameter b_j gives rise to scattering at the *same* θ, then Eq. (19.1) is replaced by

$$\frac{d\sigma}{d\Omega} = \sum_j \left|\frac{b_j}{\sin\theta\frac{d\theta}{db_j}}\right|. \tag{18.6}$$

The problem is reduced to finding θ as a function of b.

The *total cross section* σ is defined as

$$\sigma = \frac{\text{number of particles scattered per unit time}}{I}$$
$$= \int \frac{d\sigma}{d\Omega} d\Omega . \tag{18.7}$$

For any infinite range potential, the classical cross section is infinite, since particles are scattered no matter how large their impact parameter. For potentials having a finite range $r_{\max}$, $\sigma = \pi r_{\max}^2$.

Calculating θ as a function of b is a standard problem in classical mechanics. Since the potential is spherically symmetric, the orbit is in a plane perpendicular to the direction of the angular momentum and the total energy,

$$E = \frac{1}{2}\mu \dot{r}^2 + \frac{L^2}{2\mu r^2} + V(r), \tag{18.8}$$

is the sum of the potential energy and both radial and angular contributions to the kinetic energy. The *radial* motion is determined by the effective potential

$$V_{\text{eff}}(r) = V(r) + \frac{L^2}{2\mu r^2}, \tag{18.9}$$

already discussed in Chaps. 9 and 10.

Equation (18.8) can be integrated directly to obtain r as a function of t or of the scattering angle θ; however, I need to distinguish the *scattering angle* θ measured in the laboratory from the *deflection angle* Θ, which is the final value of the orbit angle relative to the z-axis (see Fig. 18.2). The scattering angle is always restricted to lie between 0 and π. If the potential is repulsive, the deflection angle must also be between 0 and π since the particle either goes straight through or is deflected away from the scattering center. In this case the scattering and deflection angles are identical. For attractive potentials, the particle is attracted so the deflection angle is negative (remember Apollo 13). Moreover the attraction can be so great that

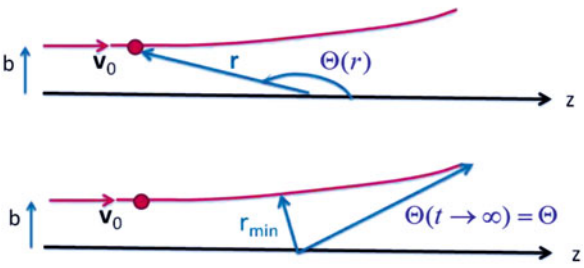

Fig. 18.2 At any point in the scattering the orbit angle can be considered as a function of the radial distance r. The final value of the orbit angle as $t \sim \infty$ is designated as the deflection angle

the deflection angle can even approach negative infinity under certain conditions (orbiting). The relation between the two angles is given by

$$\begin{aligned}
\theta &= |\Theta|\,; && -\pi \le \Theta \le \pi\,;\\
\theta &= \Theta + 2q\pi\,; && -2q\pi \le \Theta \le (-2q+1)\,\pi\,;\\
\theta &= -\Theta - 2q\pi\,; && -(2q+1)\,\pi \le \Theta \le -2q\pi\,,
\end{aligned} \tag{18.10}$$

where q is a non-negative integer. Since $d\Theta/db = \pm d\theta/db$ and $\sin\Theta = \pm\sin\theta$, θ can be replaced by Θ in Eq. (18.5).

In any scattering problem involving a spherically symmetric potential, there is a radius of closest approach $r = r_{\min}$ about which the orbit is symmetric. The time origin is chosen such that $t = 0$ when $r = r_{\min}$. For spherically symmetric potentials the orbit is in a plane perpendicular to $\mathbf{L}$ and the orbit at any time can be specified by the radial coordinate and the orbit angle Θ, which can be taken to be a function of time or radial coordinate. Since the orbit is symmetric about $r = r_{\min}$, $\Theta(r)$ is a double valued function of r; for each value of r, there are two values of Θ. However, if you restrict r such that $r < r_{\min}$ or $r > r_{\min}$, it becomes a single-valued function. The particle is incident along the *negative* z-axis at $t = -\infty$, with $\Theta(r \to \infty, t \to -\infty) = \pi$. Owing to the symmetry of the orbit

$$\begin{aligned}
\Theta(r = r_{\min}, t = 0) &= \pi + \frac{\Theta(r \to \infty, t \to \infty) - \pi}{2}\\
&= \frac{\pi + \Theta}{2},
\end{aligned} \tag{18.11}$$

where

$$\Theta \equiv \Theta(r \to \infty, t \to \infty) \tag{18.12}$$

is the deflection angle (see Fig. 18.2).

Equation (18.8) can be solved to yield

$$\dot{r} = \pm\sqrt{\frac{2}{\mu}}\sqrt{E - \frac{L^2}{2\mu r^2} - V(r)} \tag{18.13}$$

with

$$L = -\mu r^2\dot{\Theta} \tag{18.14}$$

(note that $\dot{r} < 0$ for $r < r_{\min}$, $\dot{r} > 0$ for $r > r_{\min}$, and $\dot{\Theta} < 0$). Therefore, for $r > r_{\min}$

$$\frac{d\Theta}{dr} = \frac{\dot{\Theta}}{\dot{r}} = \frac{-L}{\mu r^2\sqrt{\frac{2}{\mu}}\sqrt{E - \frac{L^2}{2\mu r^2} - V(r)}}. \tag{18.15}$$

Since Θ is a single-valued function of r for $r > r_{\min}$, I can integrate Eq. (18.15) to obtain

$$\Theta - \Theta(r = r_{\min}) = -\frac{L}{\sqrt{2\mu}} \int_{r_{\min}}^{\infty} \frac{dr}{r^2 \sqrt{E - \frac{L^2}{2\mu r^2} - V(r)}};$$

$$\Theta - \left[\frac{\pi + \Theta}{2}\right] = -\frac{L}{\sqrt{2\mu}} \int_{r_{\min}}^{\infty} \frac{dr}{r^2 \sqrt{E - \frac{L^2}{2\mu r^2} - V(r)}};$$

$$\Theta = \pi - 2b \int_{r_{\min}}^{\infty} \frac{dr}{r^2 \sqrt{1 - \frac{b^2}{r^2} - \frac{V(r)}{E}}}, \tag{18.16}$$

where Eq. (18.1b) was used.

As an example, consider scattering from a hard sphere having radius a (see Fig. 18.3), for which $r_{\min} = a$ and $V(r) = 0$ for $r > a$. Then, for $b < a$

$$\Theta = \pi - 2b \int_{a}^{\infty} \frac{dr}{r^2 \sqrt{1 - \frac{b^2}{r^2}}} = 2\cos^{-1}(b/a), \tag{18.17}$$

which can also be read from the figure. For $b > a$, $\Theta = 0$. With

$$\frac{d\Theta}{db} = -\frac{2}{a\sqrt{1 - (b/a)^2}}; \tag{18.18a}$$

$$\sin\Theta = 2\cos\frac{\Theta}{2}\sin\frac{\Theta}{2} = 2\frac{b}{a}\sqrt{1 - \frac{b^2}{a^2}}, \tag{18.18b}$$

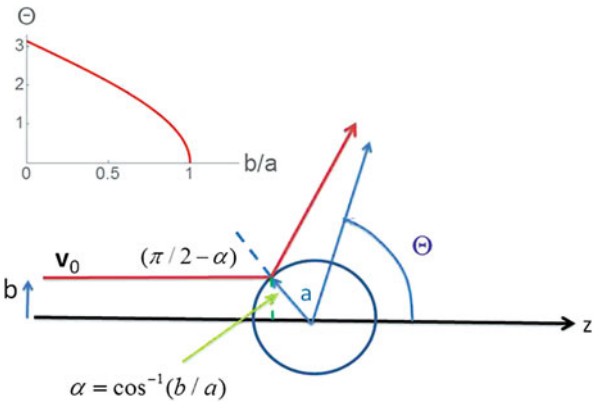

Fig. 18.3 Hard sphere scattering. The graph insert shows the deflection angle as a function of impact parameter

it follows that

$$\frac{d\sigma}{d\Omega} = \left| \frac{b}{\sin\Theta \frac{d\Theta}{db}} \right|$$
$$= \frac{b}{\frac{2b}{a}\sqrt{1-(b/a)^2}\frac{2}{a\sqrt{1-(b/a)^2}}} = \frac{a^2}{4}. \tag{18.19}$$

The scattering is isotropic! Moreover the total cross section is

$$\sigma = \int \frac{d\sigma}{d\Omega} d\Omega = \frac{a^2}{4} \int d\Omega = \frac{a^2}{4} 4\pi = \pi a^2, \tag{18.20}$$

as expected.

To discuss arbitrary potentials, it is useful to look at the effective potential. Remember that

$$L = \sqrt{2\mu E} b; \tag{18.21}$$

for a given energy, *specifying the angular momentum is equivalent to specifying the impact parameter*. Using the effective potential for scattering problems is a little different than using it for bound state problems, as I did in Chap. 10. In bound state problems, the radial motion is restricted between a minimum and maximum radius. In scattering problems, however, the particle is incident from $r = \infty$, enters the scattering region, reaches a minimum radial distance $r = r_{\min}$, and then exits the scattering region with its radial distance again approaching $r = \infty$ as $t \sim \infty$. Remember that the effective potential is for the *radial motion only* and does not give a complete description of the orbit. At $r = r_{\min}$, $\dot{r} = 0$ and all contributions to the kinetic energy of the particle come from the angular motion.

Let us first look at the case where there is *no* potential. Of course, there is no preferred origin in this problem, but we can pick one at random. For a free particle the path is a straight line having impact parameter b relative to the origin, as shown in Fig. 18.4. However, relative to this arbitrarily chosen origin, the particle has both a radial and angular contribution to its kinetic energy if $L \neq 0$ (both the radial distance and polar angle of the particle vary during its motion). The effective potential for a free particle is

$$V_{\text{eff}} = \frac{L^2}{2\mu r^2} = \frac{Eb^2}{r^2}. \tag{18.22}$$

and the minimum radial distance is

$$r_{\min} = \sqrt{\frac{L^2}{2\mu E}} = b. \tag{18.23}$$

These features are seen clearly in Fig. 18.4.

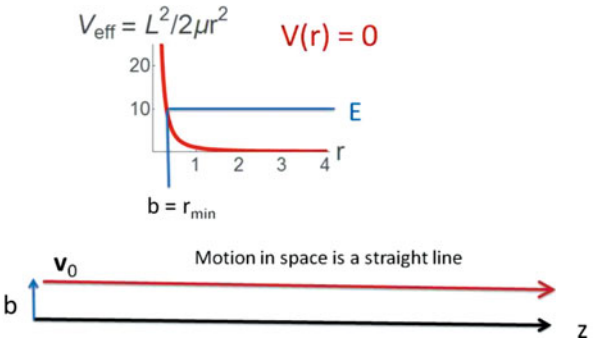

Fig. 18.4 "Scattering" in the absence of a potential. The effective potential is shown for $L \neq 0$. The minimum radius is $r_{\min} = b$. In coordinate space, the particle path in space is a straight line parallel to the z-axis

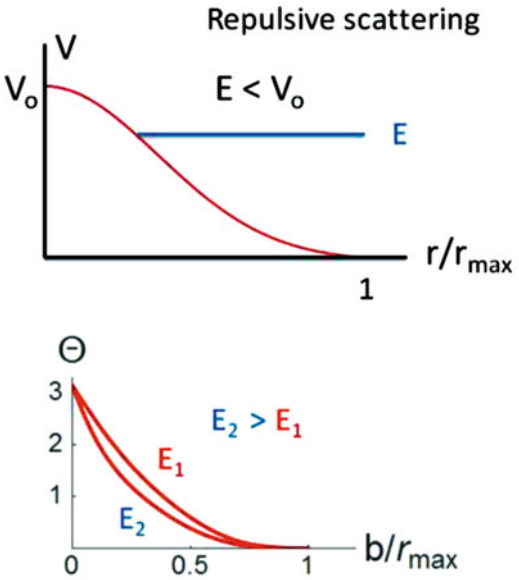

Fig. 18.5 Scattering by a finite range repulsive potential when the energy is less than the maximum of the potential

Next consider scattering by a monotonically decreasing repulsive potential having finite range $r_{\max}$, such as that shown in Fig. 18.5, when the energy E of the particle is *less* than the maximum height V_0 of the potential. In this case, for $b = 0$ ($L = 0$) the particle is repelled by the potential and goes back along its original direction, $\Theta = \pi$. With increasing impact parameter b, the strength of the potential and the scattering angle decreases monotonically, ultimately reaching zero when the impact parameter is larger than the range $r_{\max}$. If $b > r_{\max}$, the particle moves on a

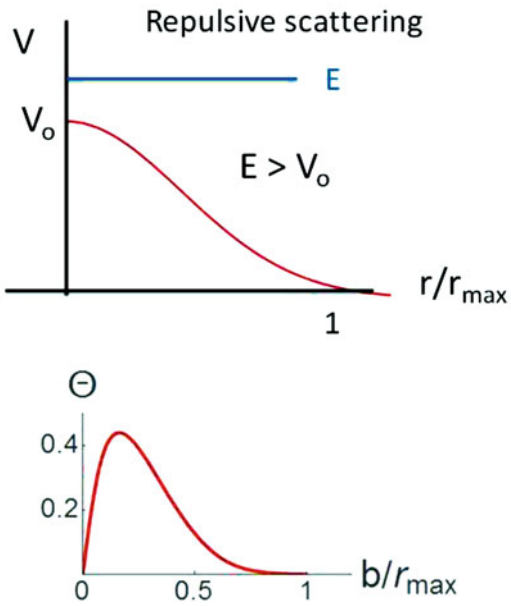

Fig. 18.6 Scattering by a finite range repulsive potential when the energy is greater than the maximum of the potential

straight line and does not encounter the potential at all. Graphs of Θ as a function of b are shown in Fig. 18.5. For a given impact parameter $b < r_{\max}$ the deflection angle decreases with increasing energy, as would be expected.

The scattering is more interesting when the energy is greater than the maximum of the potential energy (see Fig. 18.6). In this case, for $b = 0$ ($L = 0$) the particle slows down when it reaches the potential, passes through the origin, and speeds up as it leaves the potential; the deflection angle is $\Theta = 0$. But the scattering angle must also go to zero when the impact parameter is larger than the range $r_{\max}$ of the potential. As a consequence, the scattering angle must pass through a maximum. A graph of Θ as a function of b is shown in Fig. 18.6. Since $d\Theta/db = 0$ at some scattering angle, the differential scattering cross section becomes *infinite* at this impact parameter, analogous to *rainbow scattering* (actually rainbow scattering actually depends on the *wave* nature of light—see below).

For attractive potentials new features appear in the scattering since the effective potential is no longer a monotonic function of r. I will assume that the potential falls off faster than $1/r^2$ for large r and that the potential is finite at $r = 0$. With these restrictions, the effective potential for different values of angular momentum takes on the general structure indicated in Fig. 18.7. It is positive at $r = 0$ (except for $L = 0$) and also positive as $r \to \infty$ (except for $L = 0$). For sufficiently small values of $L = \sqrt{2\mu E}b \neq 0$ there is a *maximum* in the effective potential (see Fig. 18.7),

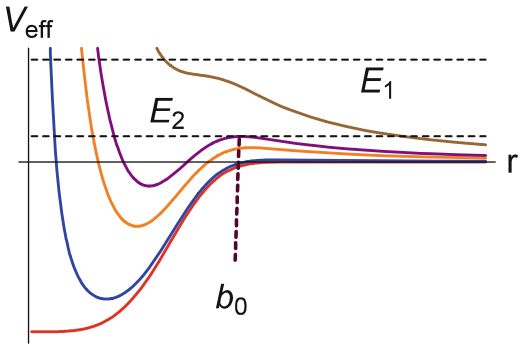

Fig. 18.7 Effective potentials for an attractive potential. The lowest curve is for $L = 0$ and each subsequent curve corresponds to a higher value of angular momentum. For sufficiently large L, there is no longer a local maximum

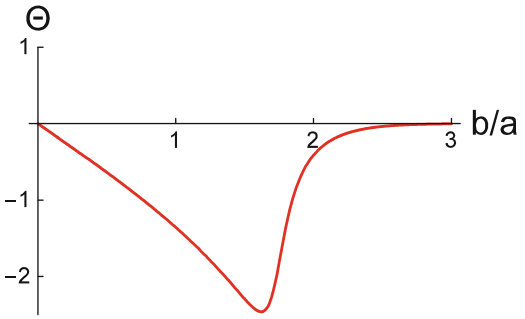

Fig. 18.8 Deflection angle for the attractive Gaussian potential of Eq. (18.24) for $V_0/E = 4$, corresponding to an energy such as E_1 shown in Fig. 18.7

but for larger values of L, no maximum occurs and the effective potential simply decays monotonically.

How is a particle scattered by such a potential? For impact parameter $b = 0$ ($L = 0$) the particle passes through the origin, $\Theta = 0$. The deflection angle also goes to zero for large values of b, but from *negative* values, since the potential is attractive. For intermediate values of b, the nature of the scattering depends on the energy of the incoming particle. For an energy such as E_1 shown in Fig. 18.7 there is *no* value of the angular momentum for which the energy intersects the effective potential at a local maximum. In this limit, a graph of the deflection angle versus impact parameter is shown in Fig. 18.8 for a potential of the form

$$V(r) = -V_0 e^{-r^2/a^2}. \tag{18.24}$$

There is rainbow-like scattering where $d\Theta/db = 0$, as there was for repulsive scattering with $E > V_0$.

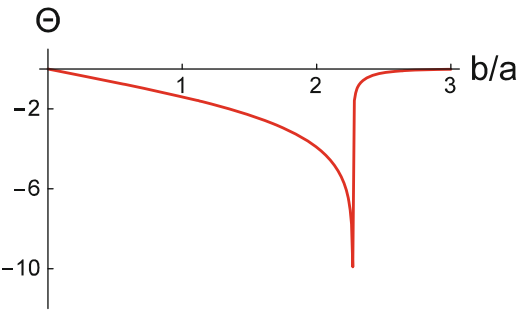

Fig. 18.9 Deflection angle for the attractive Gaussian potential of Eq. (18.24) for $V_0/E = 16$, corresponding to an energy such as E_2 shown in Fig. 18.7. Orbiting occurs for $b/a = 2.27$

On the other hand, for energies such as E_2 in Fig. 18.7 there is *always* a value of angular momentum for which the energy intersects the effective potential at its local maximum. At this angular momentum or impact parameter, the particle approaches the radius $r = b_0$ corresponding to the local maximum, but it takes an *infinite* time to get there. This corresponds to *orbiting* and the deflection angle can take on infinitely many values an infinite number of times. Although the deflection angle diverges, the differential cross section is finite. In Fig. 18.9, the deflection angle Θ is plotted as a function of b/a for the potential given by Eq. (18.24) with $V_0/E = 16$. Near $b/a = 2.27$, which corresponds to the impact parameter where $dV(r)/dr = 0$ for this potential and energy, the deflection angle is greater than 12π, indicating that orbiting has occurred.[1]

When orbiting occurs, there can be several impact parameters $b \neq 0$ for which $-\Theta_N$ is an even multiple of π (forward scattering) and for which $-\Theta_N$ is an odd multiple of π (backscattering). Since the scattering angle θ is equal to either 0 or π for these values of the deflection angle Θ_N, the differential scattering cross section, $d\sigma/d\Omega = |b/(\sin\theta d\theta/db)|$, become large or even infinite at such deflection angles (depending on the value of $d\theta/db$ at these points). This enhanced scattering is referred to as *glory scattering*. Road signs have a coating that gives rise to glory backscattering; the backscattering of light from water droplets is another example of the glory effect.

Although I said that there is no longer a local maximum with increasing L for attractive potentials, there is an exception to this general result. For potentials having a sharp cutoff, such as the *spherical well potential*,

[1] If you expand the square root in the denominator of Eq. (18.16) about $r = r_{\min}$ at the impact parameter corresponding to orbiting, you will find it varies as $(r - r_{\min})$, giving a deflection angle that diverges as $\ln[(r - r_{\min})/a]$. Numerically, it is very hard to reproduce this very slow divergence. There are very special values, $V_0/E = e^2$, $B_0/E = 4$, $r_{\min}/a = \sqrt{2}$, for which the *second* derivative also vanishes when $E = E_0$; in this case, the divergence is more rapid, varying as $[(r - r_{\min})/a]^{-1/2}$.

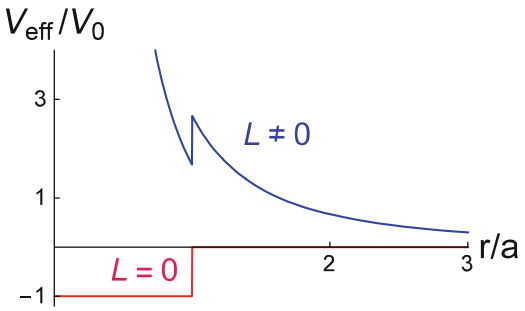

Fig. 18.10 Effective potential for a spherical well potential

$$V(r) = \begin{cases} -V_0 & r \leq a \\ 0 & r > a \end{cases}, \tag{18.25}$$

there is *always* a local maximum in the effective potential for $L \neq 0$ (see Fig. 18.10), independent of the value of L. The spherical well potential is attractive in the sense that any particle incident with impact parameter $b < a$ undergoes scattering with a negative deflection angle. It gives rise to scattering that is analogous to the scattering of electromagnetic radiation by a dielectric sphere having index of refraction,

$$n = \sqrt{1 + V_0/E}, \tag{18.26}$$

but with *no* reflections off the sphere (only transmission). For the spherical well potential, the deflection angle as a function of impact parameter can be calculated from Eq. (18.16) as

$$\Theta = 2\left[-\sin^{-1}\left(\frac{b}{a}\right) + \sin^{-1}\left(\frac{b}{na}\right)\right] \text{Heaviside}(1 - b/a), \tag{18.27}$$

where Heaviside$(x) = 1$ if $x > 0$ and is zero otherwise. The deflection angle is shown in Fig. 18.11 as a function of b/a for $n = 1.4$. The differential cross section, which can be calculated using Eqs. (18.5) and (18.27), is given by

$$\frac{d\sigma}{d\Omega} = \frac{n^2 a^2}{4\cos(\theta/2)} \frac{[n - \cos(\theta/2)]\,[n\cos(\theta/2) - 1]}{\left[1 + n^2 - 2n\cos(\theta/2)\right]^2} \times \text{Heaviside}\,[n\cos(\theta/2) - 1] \tag{18.28}$$

and vanishes for deflection angles having $\Theta < \Theta_{\text{min}} = -2\cos^{-1}(1/n)$. There is no rainbow-like or glory scattering in this classical problem.

I finish this section with a brief discussion of scattering of light rays by a dielectric sphere. In contrast to classical particle scattering by a spherical well potential, the scattering of light rays by a dielectric sphere, such as a water droplet,

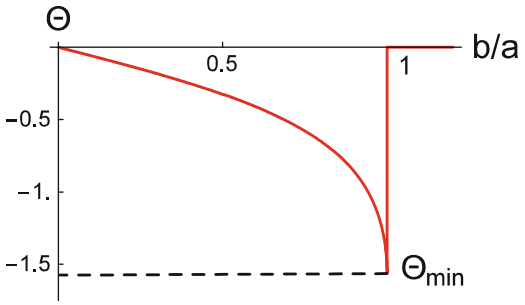

Fig. 18.11 Deflection angle for a spherical well potential with $n = \sqrt{1 + V_0/E} = 1.4$

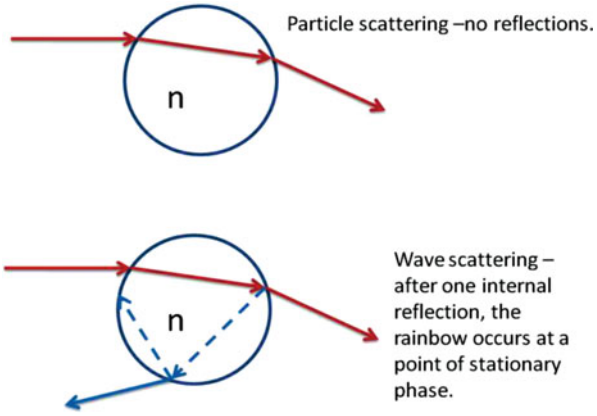

Fig. 18.12 Classical scattering by a spherical potential and rainbow scattering by a dielectric sphere (the wave reflected off the outer surface of the dielectric sphere is not shown)

can lead to rainbow and glory scattering as a result of reflections of the light on the *inner* surface of the water droplet (see Fig. 18.12). Even though the rainbow represents a geometrical optics limit for light (as does refraction at a dielectric interface), the formation of a rainbow still relies on the fact that light is a wave. Since there is a sudden change of index of refraction at the air–water droplet interface, there are wave-like effects (just as the reflection coefficient at a potential step in the quantum problem is independent of $\hbar$—it is a geometrical, wave-like effect). The scattering cross section can be thought to result from *rays* of light incident with different impact parameters. A light ray that is incident on the sphere with impact parameter b is partially reflected and partially transmitted at the outer surface of the sphere. It then undergoes an infinite number of reflections (and transmissions) on the *inner* surface of the sphere. You can show using geometric optics that the deflection angle Θ_N for the light that emerges after N reflections on the inner surface of the sphere is given by

$$\Theta_N = \left\{\left[\pi - 2\sin^{-1}(b/a)\right] - N\left[\pi - 2\sin^{-1}(b/na)\right]\right\} \text{Heaviside}(1 - b/a), \tag{18.29}$$

where n is the index of refraction of the sphere relative to the medium surrounding it. Equation (18.29) also holds for the reflection of an incoming ray off the *outer* surface of the sphere if you set $N = 0$.

For $N = 1$ the result is similar to that of classical scattering by a spherical well potential having depth V_0, with $V_0/E = n^2 - 1$—there is no contribution to rainbow or glory scattering. For $N \geq 2$, you can use Eq. (18.29) to search for contributions to rainbows (where $d\Theta_N/db = 0$) or glories (values of $-\Theta_N$ that are an integral multiple of π for $b \neq 0$). In this manner, you can show that, for $n = 4/3$ (water), the principal rainbow angle, corresponding to $N = 2$, occurs at $\Theta_N = -138°$ or 42° from the back scattering angle. Note that there is no *total* internal reflection on the inner surface, simply reflection. Contributions to glory scattering are possible for $N \geq 3$.

Equation (18.29) is also valid in the case where light goes from a higher to lower index as from scattering off an air bubble in water, provided $b/a < n$ ($n < 1$ is the relative index of refraction of the bubble to the medium surrounding the bubble). On the other hand, if $n < b/a < 1$, there is total reflection from the outer surface of the sphere with $\Theta = 2\cos^{-1}(b/a)$. In general, for $n < 1$, Eq. (18.29) is replaced by

$$\begin{aligned}\Theta_N = &\left\{\left[\pi - 2\sin^{-1}(b/a)\right] - N\left[\pi - 2\sin^{-1}(b/na)\right]\right\} \text{Heaviside}(n - b/a) \\ &+2\cos^{-1}(b/a)\text{Heaviside}(1 - b/a)\delta_{N,0}.\end{aligned} \tag{18.30}$$

In this case you can show that there is no rainbow scattering, but contributions to glories are still possible for $N \geq 3$. For $N = 0$ the result corresponds to the classical problem of scattering by a repulsive, *spherical barrier potential* when the energy of the particle is greater than the height V_0 of the well, with $V_0/E = 1 - n^2$.

18.2 Quantum Scattering

I now turn my attention to quantum scattering. This is a really important problem, since many experiments must be analyzed in terms of the differential cross sections associated with the scattering process. It is clear that quantum effects become important as soon as the scattering potential varies significantly over distances of a de Broglie wavelength of the incident particle (wave). If there is a sharp change in the potential, such as in hard sphere scattering, there are always diffraction effects. In this limit, no matter what the energy of the incident particle, there is a "wave-like" contribution to the scattering. We have already seen such effects in the scattering of a wave packet from a one-dimensional potential barrier or well. Aside from the sharp cutoff effects, there can be additional quantum effects when the de Broglie wavelength of the incident particle is comparable to distances over which the potential changes. Thus, for low energy scattering, a quantum treatment is often

needed. The rainbow-like, orbiting, and glory effects that occur for fixed impact parameters in classical scattering are "washed out" in quantum scattering since it is not possible to specify both a precise impact parameter and scattering angle owing to the uncertainty principle, but analogous processes still occur. Moreover, we will see that tunneling also occurs in certain limits, leading to very sharp resonances in the scattering.

Quantum-mechanical scattering represents a very complex problem in most cases. There are many books devoted to this subject. In this introductory presentation, I limit the discussion to scattering of structureless particles by spherically symmetric potentials. The use of the effective potential greatly aids the analysis of the problem. As for one-dimensional problems, the calculations can be given in terms of a steady-state or time-dependent approach. I will mention the time-dependent approach briefly, but concentrate on the steady-state approach. In both cases, the theory is based on the prediction (I will prove this later on) that the *asymptotic* form of the (unnormalized) eigenfunctions as $r \to \infty$ is of the form

$$\psi_k(\mathbf{r}) \sim \left(e^{ikz} + f_k(\theta)\frac{e^{ikr}}{r}\right). \tag{18.31}$$

The first term in Eq. (18.31) corresponds to a plane wave incident from the left in the positive z direction, while the second term corresponds to a *spherically scattered* wave that is weighted with the *scattering amplitude* $f_k(\theta)$. Had I carried out a time-dependent treatment, I would find that an initial wave packet having spatial extent w in the z direction and propagating in the z direction is transformed into the original wave packet propagating as if no scattering occurred, plus an outgoing *shell* having thickness w that is centered at radius $r = -z_0 + v_0 t$, where $-z_0$ is the initial location of the center of the packet and v_0 is the average speed of the initial packet. The spherical shell is weighted by $f_k(\theta)$. To arrive at this picture of the scattering, it is necessary to assume that the initial wave packet has a k-space amplitude $\Phi(\mathbf{k})$ that is sharply peaked about $\mathbf{k} = k_0\mathbf{u}_z$ and that the phase of $f_k(\theta)$ is approximately constant for values of $\mathbf{k}$ close to $k_0\mathbf{u}_z$. If the phase is not constant, but is slowly varying, there is a time delay associated with the scattering process that can depend on the scattering angle. For more rapid variations of the phase, such as those that occur near resonances, the outgoing wave packet has a complicated structure owing to dispersion associated with the phase of the scattering amplitude.

As in the 1-D case, I can get the differential scattering cross section by considering the probability current density in all but the forward direction (I return to what happens in the forward direction below). The incident probability current density is that associated with the e^{ikz} term in Eq. (18.31) and is equal to

$$\mathbf{J}_i = v_k\mathbf{u}_z = (\hbar k/\mu)\,\mathbf{u}_z, \tag{18.32}$$

where $v_k = \hbar k/\mu$. The scattered current density is that associated with the $\psi_s(\mathbf{r}) = f_k(\theta)e^{ikr}/r$ term in Eq. (18.31) and is given by

$$\mathbf{J}_s(\mathbf{r}) = \frac{i\hbar}{2\mu}\left[\psi_s(x)\nabla\psi_s^*(\mathbf{r}) - \psi_s^*(\mathbf{r})\nabla\psi_s(\mathbf{r})\right]$$
$$= \frac{i\hbar}{2\mu}\left[f_k(\theta)\frac{e^{ikr}}{r}\nabla\left\{f_k^*(\theta)\frac{e^{-ikr}}{r}\right\} - f_k^*(\theta)\frac{e^{-ikr}}{r}\nabla\left\{f_k(\theta)\frac{e^{ikr}}{r}\right\}\right]. \quad (18.33)$$

I use the expression for the gradient operator in spherical coordinates,

$$\nabla = \frac{\partial}{\partial r}\mathbf{u}_r + \frac{1}{r}\frac{\partial}{\partial\theta}\mathbf{u}_\theta + \frac{1}{r\sin\theta}\frac{\partial}{\partial\phi}\mathbf{u}_\phi, \quad (18.34)$$

to calculate

$$\nabla\left\{f_k(\theta)\frac{e^{ikr}}{r}\right\} = \left(ik - \frac{1}{r}\right)f_k(\theta)\frac{e^{ikr}}{r}\mathbf{u}_r + \frac{e^{ikr}}{r^2}\frac{df_k(\theta)}{d\theta}\mathbf{u}_\theta. \quad (18.35)$$

To get the outgoing probability flux into a solid angle $d\Omega$, I multiply $\mathbf{J}_s(\mathbf{r})$ by $r^2 d\Omega$, take the scalar product with $\mathbf{u}_r$, and let $r \to \infty$,

$$\lim_{r\to\infty} \mathbf{J}_s \cdot \mathbf{u}_r r^2 d\Omega = v_k \left|f_k(\theta)\right|^2 d\Omega. \quad (18.36)$$

The differential cross section is then calculated as

$$\frac{d\sigma}{d\Omega}d\Omega = \frac{v_k \left|f_k(\theta)\right|^2 d\Omega}{\mathbf{J}_i \cdot \mathbf{u}_z} = \left|f_k(\theta)\right|^2 d\Omega. \quad (18.37)$$

That is,

$$\frac{d\sigma}{d\Omega} = \left|f_k(\theta)\right|^2 \quad (18.38)$$

is the differential scattering cross section and

$$\sigma = \int \left|f_k(\theta)\right|^2 d\Omega = 2\pi\int_0^\pi \left|f_k(\theta)\right|^2 \sin\theta\, d\theta \quad (18.39)$$

is the total scattering cross section.

There are effectively two ways to calculate $f_k(\theta)$. One involves a formal solution of the Schrödinger equation and gives rise to the *Born series*. The second involves a solution of the radial equation for a given value of angular momentum ℓ and is referred to as the method of partial waves, for reasons to be discussed in a moment. Of course, if you can find the exact eigenfunctions for a given potential, you need only expand them for large r and compare the results with Eq. (18.31) to identify $f_k(\theta)$.

18.2.1 Method of Partial Waves

In the classical problem, for a given energy, each incident impact parameter or value of the angular momentum is associated with a single scattering angle. In quantum mechanics this picture is no longer valid since it would imply that we could simultaneously specify both the position (impact parameter) and momentum (given by the scattering angle) of the particle. Nevertheless, it is possible to write the differential scattering amplitude as arising from contributions from each value of ℓ, since ℓ is a conserved quantum number. This is the origin of the terminology, *method of partial waves.* Several (in principle, *all*) values of ℓ give rise to scattering at the same angle, and there can be interference among the various contributions. Nevertheless, it is convenient to view the quantum-mechanical scattering as arising from contributions from different impact parameters.

An uncertainty principle argument can also help you to understand why quantum total cross sections can be finite for infinite range potentials, whereas they are infinite in the corresponding classical case. The question is, when does the uncertainty principle lead to a breakdown of a classical approach. The uncertainty principle requires that the transverse momentum Δp_t imparted to the particle by the potential multiplied by the impact parameter that gives rise to this scattering must be greater than or of order $\hbar$; that is

$$b\Delta p_t \gtrsim \hbar. \tag{18.40}$$

For a potential V varying as C/r^s, the change in transverse momentum can be estimated as

$$\Delta p_t = \int F dt \approx \frac{dV}{dr}\frac{b}{v} \approx \frac{C}{b^{s+1}}\frac{b}{v} = \frac{C}{b^s}\frac{b}{v}, \tag{18.41}$$

where v is the incident speed. Therefore, the maximum impact parameter $b_{\max}$ for which a classical picture can remain valid is determined from the condition

$$b_{\max}\frac{C}{v b_{\max}^s} \approx \hbar, \tag{18.42}$$

which yields

$$b_{\max} \approx \left(\frac{C}{\hbar v}\right)^{\frac{1}{s-1}}. \tag{18.43}$$

As a consequence, we might expect that the total quantum cross section is of order

$$\pi b_{\max}^2 = \pi \left(\frac{C}{\hbar v} \right)^{\frac{2}{s-1}}, \tag{18.44}$$

a quantity that is finite for $s > 1$. Note that Eq. (18.44) predicts an infinite cross section for Coulomb scattering, which is actually the case, even quantum-mechanically. For potentials that fall off faster than $1/r$ as $r \to \infty$ there is always an *effective* maximum range of the potential given by $r_{\max} = b_{\max}$ and an associated diffractive scattering component in the differential scattering cross section that would arise from a potential having a *sharp* cut-off at $r = r_{\max}$.

To apply the method of partial waves, I must solve the Schrödinger equation exactly. This is no easy task, but at least I can solve it for large r. If I assume that the scattering potential falls off faster than $1/r^2$, the effective potential at large r is dominated by the angular momentum term—in other words, the effective potential is that of a free particle. I have considered free particle solutions in spherical coordinates in Chap. 10. The general solution for the radial wave function of a free particle for $r \neq 0$ can be written as (see Appendix 1)

$$R_\ell(r) = r u_\ell(r) = A_\ell j_\ell(kr) + B_\ell n_\ell(kr), \tag{18.45}$$

where

$$k = \sqrt{\frac{2\mu E}{\hbar^2}}, \tag{18.46}$$

are $j_\ell(kr)$ and $n_\ell(kr)$ are spherical Bessel and Neumann functions.

Thus, for spherically symmetric potentials, the solution for the wave function, valid at large r, is

$$\psi_k(\mathbf{r}) \sim \sum_{\ell=0}^{\infty} \left[A_\ell j_\ell(kr) + B_\ell n_\ell(kr) \right] P_\ell(\cos\theta). \tag{18.47}$$

Owing to the azimuthal symmetry of the scattering process about the z-axis, the wave function has no ϕ dependence, which is why the Legendre polynomials appear in the summation rather than the spherical harmonics. The actual values of A_ℓ and B_ℓ can be obtained only if you solve the radial equation *exactly* for *all* r. To obtain an expression for the scattering amplitude, I must expand Eq. (18.47) for large kr. Using the asymptotic form of the spherical Bessel and Neumann functions,

$$j_\ell(x) \sim \frac{\sin\left(x - \frac{\ell\pi}{2}\right)}{x}; \tag{18.48}$$

$$n_\ell(x) \sim \frac{-\cos\left(x - \frac{\ell\pi}{2}\right)}{x}, \tag{18.49}$$

valid for $x \gg 1$ and $x \gg \ell$, I find

$$\psi_k(\mathbf{r}) \sim \sum_{\ell=0}^{\infty} \frac{A_\ell \sin\left(kr - \frac{\ell\pi}{2}\right) - B_\ell \cos\left(kr - \frac{\ell\pi}{2}\right)}{kr} P_\ell(\cos\theta). \tag{18.50}$$

Since I have already assumed that

$$\psi_k(\mathbf{r}) \sim \left(e^{ikz} + f_k(\theta)\frac{e^{ikr}}{r}\right), \tag{18.51}$$

I must now equate Eqs. (18.50) and (18.51) to find the appropriate $f_k(\theta)$.

To do so, I first use the identity

$$e^{ikz} = e^{ikr\cos\theta} = \sum_{\ell=0}^{\infty} i^\ell (2\ell+1) j_\ell(kr) P_\ell(\cos\theta), \tag{18.52}$$

which follows from the solution of the free particle Schrödinger equation in spherical coordinates (see Appendix 1). For large kr I use the asymptotic form of the Bessel function to rewrite this equation as

$$e^{ikz} \sim \sum_{\ell=0}^{\infty} i^\ell (2\ell+1) \frac{\sin(kr - \frac{\ell\pi}{2})}{kr} P_\ell(\cos\theta). \tag{18.53}$$

I next set

$$A_\ell = D_\ell \cos\delta_\ell; \tag{18.54a}$$

$$B_\ell = -D_\ell \sin\delta_\ell; \tag{18.54b}$$

$$\tan\delta_\ell = -\frac{B_\ell}{A_\ell}, \tag{18.54c}$$

such that

$$A_\ell \sin\left(kr - \frac{\ell\pi}{2}\right) - B_\ell \cos\left(kr - \frac{\ell\pi}{2}\right) = D_\ell \sin\left(kr - \frac{\ell\pi}{2} + \delta_\ell\right). \tag{18.55}$$

The quantity δ_ℓ is referred to as a *partial wave phase*. By combining Eqs. (18.50), (18.51), (18.53), and (18.55), I find

$$\begin{aligned}\psi_k(\mathbf{r}) &\sim \frac{1}{kr}\sum_{\ell=0}^{\infty} D_\ell \sin\left(kr - \frac{\ell\pi}{2} + \delta_\ell\right) P_\ell(\cos\theta) \\ &= \frac{1}{kr}\sum_{\ell=0}^{\infty} i^\ell (2\ell+1) \sin\left(kr - \frac{\ell\pi}{2}\right) P_\ell(\cos\theta) + \frac{f_k(\theta)}{r} e^{ikr}\end{aligned} \tag{18.56}$$

or

$$f_k(\theta)e^{ikr} = \frac{1}{k}\sum_{\ell=0}^{\infty}\left[D_\ell \sin\left(kr - \frac{\ell\pi}{2} + \delta_\ell\right) - i^\ell(2\ell+1)\sin\left(kr - \frac{\ell\pi}{2}\right)\right] \times P_\ell(\cos\theta). \tag{18.57}$$

To solve this equation, I equate coefficients of $e^{\pm ikr}$ appearing on both sides of the equation. Equating coefficients of e^{-ikr} I find

$$0 = \frac{1}{k}\sum_{\ell=0}^{\infty} i^\ell\left[D_\ell e^{-i\delta_\ell} - i^\ell(2\ell+1)\right]P_\ell(\cos\theta). \tag{18.58}$$

Since θ is arbitrary, the only possible solution is

$$D_\ell = i^\ell e^{i\delta_\ell}(2\ell+1). \tag{18.59}$$

Equating coefficients of e^{ikr} then yields

$$f_k(\theta) = \frac{1}{2ik}\sum_{\ell=0}^{\infty}(-i)^\ell\left[D_\ell e^{i\delta_\ell} - i^\ell(2\ell+1)\right]P_\ell(\cos\theta). \tag{18.60}$$

Combining Eqs. (18.59) and (18.60), I obtain the scattering amplitude

$$f_k(\theta) = \frac{1}{2ik}\sum_{\ell=0}^{\infty}(2\ell+1)\left(e^{2i\delta_\ell} - 1\right)P_\ell(\cos\theta), \tag{18.61}$$

which can also be written as

$$f_k(\theta) = \frac{1}{k}\sum_{\ell=0}^{\infty}(2\ell+1)e^{i\delta_\ell}\sin(\delta_\ell)\,P_\ell(\cos\theta). \tag{18.62}$$

The problem is solved once you calculate the partial wave phases δ_ℓ.

To find the δ_ℓ, you can proceed as follows:

- For each value of ℓ, solve Schrödinger's equation *exactly* for the given potential to obtain the eigenfunctions.

- As $r \to \infty$, express the radial eigenfunctions in the form

$$\begin{aligned} u_\ell(r) &= R_\ell(r)/r = A_\ell j_\ell(kr) + B_\ell n_\ell(kr) \\ &\sim A_\ell \sin\left(kr - \frac{\ell\pi}{2}\right) - B_\ell \cos\left(kr - \frac{\ell\pi}{2}\right) \\ &= D_\ell \sin\left(kr - \frac{\ell\pi}{2} + \delta_\ell\right) \end{aligned} \tag{18.63}$$

  from which the δ_ℓ can be extracted.

Of course it is not easy to solve the Schrödinger equation for most potentials. If you need only a few partial waves, then the method of partial waves is most useful. If the range of the potential is of order a, then impact parameters of order a are needed. That is

$$b_{\max} = \frac{L_{\max}}{\mu v} \approx \frac{\hbar \ell_{\max}}{\mu v} \approx a; \tag{18.64a}$$

$$\ell_{\max} \approx \frac{\mu v a}{\hbar} = \frac{pa}{\hbar} = ka. \tag{18.64b}$$

Therefore, the partial wave expansion is especially useful when $ka \lesssim 1$. On the other hand, even for high energies, $ka \gg 1$, it is often possible to solve the radial equation using the WKB method and then extract the phase shifts. In this limit, the method of partial waves can also be used at high energies.

18.2.1.1 Differential and Total Cross Sections: Optical Theorem

Before discussing some specific examples and examining the meaning of the partial wave phases, I derive an expression for the total cross section and relate it to the scattering amplitude. In doing so, I can address the question of the nature of the scattering in the forward direction. From Eqs. (18.38) and (18.62), I find

$$\frac{d\sigma}{d\Omega} = \frac{1}{k^2}\left|\sum_{\ell=0}^{\infty}(2\ell+1)e^{i\delta_\ell}\sin\delta_\ell P_\ell(\cos\theta)\right|^2 \tag{18.65}$$

and

$$\begin{aligned} \sigma = \frac{2\pi}{k^2}\sum_{\ell,\ell'=0}^{\infty}\int_{-1}^{1} d(\cos\theta)(2\ell+1)e^{i\delta_\ell}\sin\delta_\ell P_\ell(\cos\theta)(2\ell'+1)e^{-i\delta_{\ell'}} \\ \times \sin\delta_{\ell'} P_{\ell'}(\cos\theta) \end{aligned}$$

$$= \frac{2\pi}{k^2} \sum_{\ell,\ell'=0}^{\infty} (2\ell+1) e^{i\delta_\ell} \sin\delta_\ell (2\ell'+1) e^{-i\delta_{\ell'}} \sin\delta_{\ell'} \frac{2\delta_{\ell,\ell'}}{(2\ell+1)}$$

$$= \frac{4\pi}{k^2} \sum_{\ell=0}^{\infty} (2\ell+1) \sin^2\delta_\ell. \tag{18.66}$$

Since $P_\ell(1) = P_\ell[\cos(\theta = 0)] = 1$, this can be re-expressed as

$$\sigma = \frac{4\pi}{k} \operatorname{Im}\left[\frac{1}{k} \sum_{\ell=0}^{\infty} (2\ell+1) e^{i\delta_\ell} \sin\delta_\ell P_\ell(\cos 0)\right]$$

$$= \frac{4\pi}{k} \operatorname{Im} f_k(0), \tag{18.67}$$

which is known as the *optical theorem*. It relates the total cross section to the forward scattering amplitude. What is the physical meaning of this equation?

Some insight into the answer to this question can be obtained by returning to the asymptotic form of the wave function

$$\psi_k(\mathbf{r}) \sim \left(e^{ikz} + f_k(\theta)\frac{e^{ikr}}{r}\right). \tag{18.68}$$

The initial probability current density is

$$\mathbf{J}_i = \frac{\hbar k}{\mu}\mathbf{u}_z \tag{18.69}$$

and the final probability current density is

$$\mathbf{J}_f = \frac{i\hbar}{2\mu}\left[e^{ikz} + f_k(\theta)\frac{e^{ikr}}{r}\right]$$
$$\times\left[-ike^{-ikz}\mathbf{u}_z - f_k^*(\theta)\frac{e^{-ikr}}{r}\left(ik + \frac{1}{r}\right)\mathbf{u}_r + \frac{e^{-ikr}}{r^2}\frac{df_k^*(\theta)}{d\theta}\mathbf{u}_\theta\right]$$
$$+\text{c.c.}$$
$$= \frac{\hbar k}{\mu}\mathbf{u}_z + \frac{\hbar k}{\mu}\frac{|f_k(\theta)|^2}{r^2}\mathbf{u}_r$$
$$+\left\{\frac{i\hbar}{2\mu}\left[e^{ikz} + f_k(\theta)\frac{e^{ikr}}{r}\right]\frac{e^{-ikr}}{r^2}\frac{df_k^*(\theta)}{d\theta}\mathbf{u}_\theta + \text{c.c.}\right\}$$

$$+\frac{\hbar k}{2\mu}\left[e^{-ikz}f_k(\theta)\frac{e^{ikr}}{r}\mathbf{u}_z+\text{c.c.}\right]$$
$$+\frac{\hbar k}{2\mu}\left[e^{ikz}f_k^*(\theta)\left(1+\frac{1}{ikr}\right)\frac{e^{-ikr}}{r}\mathbf{u}_r+\text{c.c.}\right]. \tag{18.70}$$

For probability to be conserved, the *change* in the normal component of the probability density integrated over a spherical surface must vanish as the radius R of the sphere approaches infinity. Using the facts that $z = r\cos\theta$, $\mathbf{u}_z{\cdot}\mathbf{u}_r = \cos\theta$, $\oint \cos\theta d\Omega = 0$, $\mathbf{u}_r{\cdot}\mathbf{u}_\theta = 0$, $d\Omega = d\phi d(\cos\theta)$, and carrying out the integration over ϕ, I find

$$0 = \frac{\mu}{\hbar k}\lim_{R\to\infty}\oint R^2 d\Omega\left(\mathbf{J}_f-\mathbf{J}_i\right)\cdot\mathbf{u}_r = \int d\Omega\,|f_k(\theta)|^2 + 2\pi$$
$$\times\lim_{R\to\infty}\int_{-1}^{1} d(\cos\theta)\left\{\begin{array}{c}\frac{R}{2}\left[e^{-ikR\cos\theta}\cos\theta f_k(\theta)e^{ikR}+\text{c.c.}\right]\\ +\frac{R}{2}\left[e^{ikR\cos\theta}f_k^*(\theta)\left(1+\frac{1}{ikR}\right)e^{-ikR}+\text{c.c.}\right]\end{array}\right\}. \tag{18.71}$$

There are two types of terms, the first involves the radial flow of the scattered wave and the second and third represent interference of the incident and scattered waves. Integrating the second and third terms by parts, I obtain

$$\int d\Omega\,|f_k(\theta)|^2 + \pi\left[\frac{f_k(0)+f_k(\pi)e^{-2ikR}}{-ik}+\text{c.c.}\right]$$
$$+\pi\left[\frac{f_k^*(0)-f_k^*(\pi)e^{2ikR}}{ik}+\text{c.c.}\right]=0. \tag{18.72}$$

Additional terms in the integration by parts are neglected since they vanish in the limit $R\to\infty$. The $e^{\pm 2ikR}$ terms cancel and I am left with

$$\sigma = \int d\Omega\,|f_k(\theta)|^2 = \frac{2\pi}{ik}\left[f_k(0)-f_k^*(0)\right] = \frac{4\pi}{k}\,\text{Im}f_k(0). \tag{18.73}$$

This result now has a very simple physical interpretation. The incident wave (or wave packet) is scattered in all directions. In the forward direction the incident wave *interferes* with the scattered wave to reduce the probability current in the forward direction in precisely the amount that corresponds to scattering in all the other directions. In other words, the optical theorem is just a statement of conservation of probability.

18.2.1.2 Interpretation of the Partial Wave Phases

There is also a simple interpretation that can be given to the partial wave phases. For a free particle

$$R_\ell(r) = j_\ell(kr) \sim \frac{\sin\left(kr - \frac{\ell\pi}{2}\right)}{kr} \tag{18.74}$$

as $r \to \infty$. For a particle scattered by a potential, $\sin\left(kr - \frac{\ell\pi}{2}\right)$ is replaced by $\sin\left(kr - \frac{\ell\pi}{2} + \delta_\ell\right)$ [see Eqs. (18.50) and (18.55)]. Thus the partial wave phases are simply phase *shifts* in the asymptotic wave function produced by the potential. For example, for an infinitely repulsive hard sphere potential having radius a, the wave function is displaced from the origin. For $\ell = 0$ it is displaced by a, giving rise to a phase shift $\delta_0 = -ka$. For higher ℓ, the shift depends on ℓ but is always negative. Any purely repulsive potential always produces negative phase shifts, analogous to the fact that classical repulsive scattering always leads to positive deflection angles.

For scattering by attractive potentials, new and interesting phenomena can occur. The phase shifts are positive, in general, because the wave function is pulled in by the potential, but for strong potentials the wave function can be pulled in so much that an extra oscillation occurs and gives rise to negative phase shifts of the type you would normally associate with a repulsive interaction. Although the deflection angle is negative for classical scattering by attractive potentials, deflection angles such as those satisfying $-\pi < \Theta < -2\pi$ correspond to scattering that can mimic that of a repulsive potential. It is often stated that the interatomic potential in Bose condensates is repulsive since repulsive interactions are needed to produce the condensates. Actually the true interaction is attractive, but the *effective* interaction is repulsive.

There is another interpretation that can be given to the phase shifts that is valid for large energy and angular momenta. The radial wave equation for $u_\ell(r) = rR_\ell(r)$ is

$$\frac{d^2u_\ell}{dr^2} + k^2u_\ell - \frac{2\mu V(r)u_\ell}{\hbar^2} - \frac{\ell\,(\ell+1)}{r^2}u_\ell = 0. \tag{18.75}$$

Asymptotically, as $r \to \infty$,

$$u_\ell(r) \sim \sin\left(kr - \frac{\ell\pi}{2} + \delta_\ell\right). \tag{18.76}$$

Equation (18.75) can be solved using the WKB method in the limit of high energies and high angular momentum, since the effective potential does not vary significantly over a de Broglie wavelength in this limit. By solving Eq. (18.75) as I did in Chap. 16, you can show that the WKB wave function for $r > a$, where a is the classical turning point, is given by

$$u_\ell^{WKB}(r) = \frac{C}{\sqrt{k(r)}} \sin\left[\int_a^r k(r')dr' + \pi/4\right] \tag{18.77}$$

where C is a constant and

$$k(r) = \sqrt{k^2 - \frac{2\mu V(r)}{\hbar^2} - \frac{\ell\,(\ell+1)}{r^2}}$$
$$= \sqrt{\frac{2\mu}{\hbar^2}}\sqrt{E - V(r) - \frac{\hbar^2\ell\,(\ell+1)}{2\mu r^2}}. \tag{18.78}$$

As $r \to \infty$, the radial function can be written as

$$u_\ell^{WKB}(r) = \frac{C}{\sqrt{k(r)}}\sin\left[kr + \int_a^\infty dr'\left[k(r') - k\right] - ka + \pi/4\right]. \tag{18.79}$$

By comparing Eqs. (18.76) and (18.79), you can see that the partial wave phase shift is given by

$$\delta_\ell^{WKB} = \frac{\ell\pi}{2} + \int_a^\infty dr\left[k(r') - k\right] - ka + \pi/4$$
$$= \frac{\ell\pi}{2} + \sqrt{\frac{2\mu E}{\hbar^2}}\int_a^\infty dr\left(\sqrt{1 - \frac{V(r)}{E} - \frac{\hbar^2\ell\,(\ell+1)}{2\mu E r^2}} - 1\right)$$
$$-ka + \pi/4. \tag{18.80}$$

For a classical limit in which $\ell \gg 1$, $\ell\,(\ell+1) \approx \ell^2$, the derivative of the phase shift with respect to ℓ is given by

$$\frac{d}{d\ell}\delta_\ell^{WKB} \approx \frac{\pi}{2} - \hbar^2\ell\sqrt{\frac{1}{2\mu E\hbar^2}}\int_a^\infty \frac{dr}{r^2\left(\sqrt{1 - \frac{V(r)}{E} - \frac{\hbar^2\ell^2}{2\mu E r^2}}\right)}. \tag{18.81}$$

If I set $L = \hbar\ell = \mu v b = \sqrt{2\mu E}b$ and compare Eq. (18.81) with Eq. (18.16), I find

$$2\frac{d}{d\ell}\delta_\ell^{WKB} = \pi - 2b\int_a^\infty \frac{dr}{r^2\sqrt{1 - \frac{b^2}{r^2} - \frac{V(r)}{E}}} = \Theta; \tag{18.82}$$

the derivative of the phase shift is related to the deflection angle for scattering with impact parameter b! Using this approximation, one can show that it is possible to recover the classical limit for the differential scattering cross section in the high energy limit.

18.2.1.3 Calculation of the Partial Phase Shifts

I consider only two examples: scattering by a hard sphere and scattering by a spherical well potential, but first I discuss some general qualitative features of the partial wave approach. The scattering associated with the first few partial waves is designated by the standard letter scheme of angular momentum. Thus, $\ell = 0$ corresponds to S wave scattering, $\ell = 1$ to P wave scattering, $\ell = 2$ to D wave scattering, etc. The largest angular momentum quantum number $\ell_{\max}$ that can be expected to contribute to the sum over ℓ for scattering by a potential having finite range $r_{\max}$ is

$$\ell_{\max} = \frac{L_{\max}}{\hbar} = \frac{\mu v r_{\max}}{\hbar} \approx \frac{r_{\max}}{\lambda_{dB}} \approx k r_{\max}. \tag{18.83}$$

At low energies, $kr_{\max} \ll 1$, only S wave scattering is important. In that case

$$\frac{d\sigma}{d\Omega} \approx \frac{\sin^2 \delta_0}{k^2}; \tag{18.84a}$$

$$\sigma = \frac{4\pi \sin^2 \delta_0}{k^2} = \frac{\sin^2 \delta_0}{\pi} \lambda_{dB}^2. \tag{18.84b}$$

The scattering is isotropic and, since the de Broglie wavelength is larger than the scattering range, the incoming wave "surrounds" the scattering center and is scattered by the total surface area of the potential rather than the cross-sectional area.

In the opposite limit of high energy scattering, where

$$\ell_{\max} = \frac{L_{\max}}{\hbar} = \frac{\mu v r_{\max}}{\hbar} \approx \frac{r_{\max}}{\lambda_{dB}} \approx k r_{\max} \gg 1, \tag{18.85}$$

many partial waves contribute to the scattering. One can convert the sum over ℓ to an integral over impact parameters. For each impact parameter, there is a scattering angle that corresponds to the maximum contribution to the integral (point of stationary phase). In some sense, we recapture the classical limit in which scattering at a given impact parameter gives rise to scattering at a particular angle. The calculation is reminiscent of the Feynman path integral approach where the classical path makes the major contribution to an integral of the action between two fixed points. There is a difference from the classical case however, since contributions from different ℓ can interfere, giving rise to rapid oscillations in the differential cross section as a function of angle—it is only when these oscillations are assumed to average to zero (as would be the case if an experiment could not resolve the oscillations as a function of angle) does one recover the classical limit of the differential cross section.

Hard Sphere Scattering

I first consider the hard sphere potential

$$V(r) = \begin{cases} \infty & r \le a \\ 0 & r > a \end{cases}. \tag{18.86}$$

Recall that in the classical case, the differential scattering cross section is $a^2/4$ (isotropic) and the total cross section is πa^2. The maximum impact parameter giving rise to scattering is $b_{\max} = a$. For an incident energy $E = \mu v^2/2$, there is no scattering for $L > \mu v a$. In the quantum problem we would expect that partial waves having $\ell < \mu v a/\hbar = ka$ provide the major contribution to the scattering.

In the quantum problem, the radial wave function vanishes for $r \le a$. For $r > a$ the potential is that of a free particle, giving a general solution

$$R_\ell(r) = A_\ell j_\ell(kr) + B_\ell n_\ell(kr). \tag{18.87}$$

The radial wave function must vanish at $r = a$, leading to the condition

$$0 = A_\ell j_\ell(ka) + B_\ell n_\ell(ka) \tag{18.88}$$

or

$$\tan\delta_\ell = -\frac{B_\ell}{A_\ell} = \frac{j_\ell(ka)}{n_\ell(ka)}. \tag{18.89}$$

Some care must be used in interpreting δ_ℓ if you use a computer program to evaluate it, since most programs return the principal value of $\tan^{-1}$.

On the other hand there is no ambiguity in calculating the value of $\sin\delta_\ell$ using $\delta_\ell = \tan^{-1}[j_\ell(ka)/n_\ell(ka)]$. The result is

$$\sin\delta_\ell = \frac{j_\ell(ka)}{\sqrt{[j_\ell(ka)]^2 + [n_\ell(ka)]^2}}. \tag{18.90}$$

As a consequence, the differential cross section can then be obtained using Eq. (18.65) as

$$\frac{d\sigma}{d\Omega} = \frac{1}{k^2}\left|\sum_{\ell=0}^{\infty}(2\ell+1)e^{i\tan^{-1}\left(\frac{j_\ell(ka)}{n_\ell(ka)}\right)}\frac{j_\ell(ka)}{\sqrt{[j_\ell(ka)]^2 + [n_\ell(ka)]^2}}P_\ell(\cos\theta)\right|^2, \tag{18.91}$$

and the total cross section using Eq. (18.66) as

$$\sigma = \frac{4\pi}{k^2}\sum_{\ell=0}^{\infty}(2\ell+1)\frac{[j_\ell(ka)]^2}{[j_\ell(ka)]^2+[n_\ell(ka)]^2}. \tag{18.92}$$

Recall that $\lambda_{dB} = 2\pi/k$ and $k^2 = 2\mu E/\hbar^2$, such that

$$ka = 2\pi\frac{a}{\lambda_{dB}} = \sqrt{\frac{2\mu E a^2}{\hbar^2}} \tag{18.93}$$

is a dimensionless measure of the energy. If $ka \ll 1$, the de Broglie wavelength is larger than the scattering radius and quantum effects are important. For $ka \gg 1$ you might expect that the quantum result reduces to the classical one, but this is only partially true. Let me analyze the scattering in the low and high energy regions, $ka \ll 1$ and $ka \gg 1$, respectively.

Low Energy - $ka \ll 1$

In this limit, only $\ell = 0$ contributes significantly. For $\ell = 0$,

$$\tan\delta_0 = \frac{\sin(ka)}{-\cos(ka)} = -\tan ka; \tag{18.94a}$$

$$\delta_0 = -ka, \tag{18.94b}$$

the wave is shifted so that there is a node in the radial wave function at $r = a$. As I already mentioned, the radial wave function is displaced by a distance a when $\ell = 0$ for hard sphere scattering. The differential and total cross sections are given approximately by

$$\frac{d\sigma}{d\Omega} \approx \frac{1}{k^2}\frac{[j_0(ka)]^2}{[j_0(ka)]^2+[n_0(ka)]^2} = \frac{\sin^2(ka)}{k^2} \approx a^2; \tag{18.95a}$$

$$\sigma \approx 4\pi a^2. \tag{18.95b}$$

The scattering is isotropic and the total cross section is four times the geometrical one—in some sense the wave "sees" the entire surface area of the sphere, instead of just the cross section.

High Energy - $ka \gg 1$

In this limit, values of $\ell \lesssim ka$ contribute to the cross section. For $ka \gg 1$, the differential and total cross sections can be approximated by methods that are discussed in Appendix 2. Near $\theta = 0$, there is a peak resulting from *diffractive scattering* at the sharp boundary of the hard sphere. For larger θ, the differential cross section settles down to a value close to the classical limit of $a^2/4$. The diffraction peak has an amplitude of order

$$\frac{d\sigma\,(\theta=0)}{d\Omega} \approx \frac{a^2}{4}\,(ka)^2\,, \tag{18.96}$$

width of order $\Delta\theta \approx 4/ka$, and contributes πa^2 to the total cross section. The classical part of the scattering also contributes πa^2 to the total cross section, such that the total cross section is

$$\sigma = 2\pi a^2, \tag{18.97}$$

twice the classical limit. This is another example where a sharp change in the potential gives rise to a wave effect, regardless of the incident energy. Of course you never see such diffractive scattering in classical experiments since you would have to prepare a coherent wave to scatter off another particle. In some laser spectroscopy experiments, evidence for diffractive scattering of Yb (atomic mass =178) was shown explicitly.[2] Diffractive scattering also contributes significantly to the diffusion coefficients of atoms in vapors.

For arbitrary ka, you can simply use Eq. (18.89) to evaluate the phase shifts and then carry out the sums in Eqs. (18.65) and (18.66) to obtain the differential and total cross sections. This may take some time to do on a computer, but not that long if $ka < 100$. Some graphs are shown in Figs. 18.13, 18.14 and 18.15, the last of which corresponds to high energy scattering, where the forward scattering diffractive peak is seen clearly. A graph $\sigma/\pi a^2$ as a function of ka is shown in Fig. 18.16. The cross section varies from $4\pi a^2$ in the low energy limit to $2\pi a^2$ in the high energy limit.

Scattering by a Spherical Potential Well

I now consider scattering by the spherical well potential

$$V(r) = \begin{cases} -V_0 & r \le a \\ 0 & r > a \end{cases}. \tag{18.98}$$

Although I concentrate mainly on the case of positive V_0, the analysis is equally valid for a spherical barrier potential, with $V_0 < 0$. This is an extraordinarily rich problem and I cannot discuss many aspects of the solution, but you can examine the numerical solutions at your leisure. In this case, many features of the scattering are *not* related to the sharp discontinuity in the potential; they occur for *any* finite range potential. That is what makes a study of the spherical well potential so important.

Recall that in the corresponding case of electromagnetic scattering by a dielectric sphere, there were many interesting effects possible, such as rainbow and glory

[2] See, for example, R. A. Forber, L. Spinelli, J. E. Thomas, and M. S. Feld, *Observation of Quantum Diffractive Velocity-Changing Collisions by Use of Two-Level Heavy Optical radiators*, Physical Review Letters **50**, 331–334 (1983).

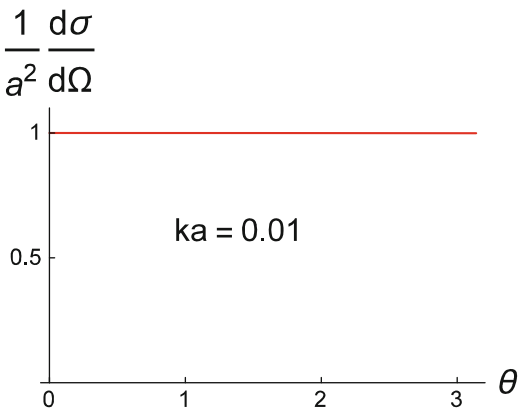

Fig. 18.13 Hard sphere scattering for $ka = 0.01$. The total scattering cross section is $\sigma = 4.0\pi a^2$

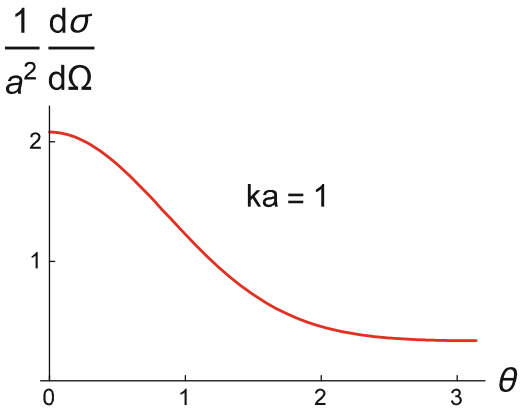

Fig. 18.14 Hard sphere scattering for $ka = 1$. The total scattering cross section is $\sigma = 3.4\pi a^2$

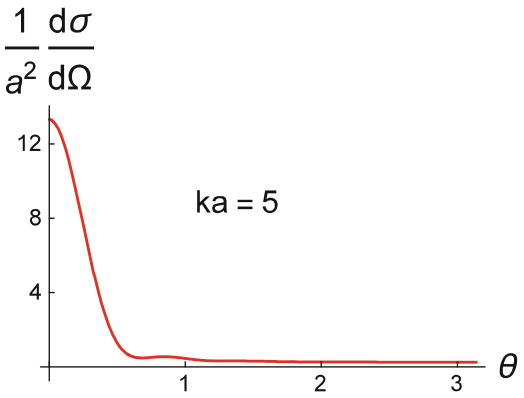

Fig. 18.15 Hard sphere scattering for $ka = 5$, showing a forward diffraction peak and isotropic scattering outside the peak. The total scattering cross section is $\sigma = 2.6\pi a^2$

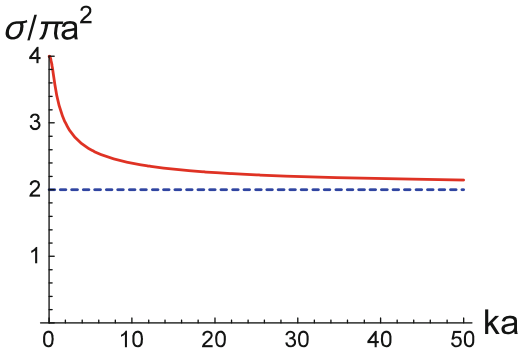

Fig. 18.16 Total cross section σ (in units of πa^2) as a function of ka for hard sphere scattering. At high energies the cross section approaches $\sigma/\pi a^2 \sim 2$, twice the classical value

scattering. We can try to look for some of these effects in the quantum case. The maximum impact parameter giving rise to scattering is $b_{\max} = a$ in the classical problem so, as in the case of hard sphere scattering, we can expect that partial waves having $\ell \lesssim ka$ to provide the major contribution to the scattering.

The potential is constant for both $r < a$ and $r > a$, but the radial wave function must be finite as $r \to 0$. As such, the general solution for the radial wave function is

$$R_\ell(r) = \begin{cases} C_\ell j_\ell(k_1 r) & r < a \\ A_\ell j_\ell(kr) + B_\ell n_\ell(kr) & r > a \end{cases}, \tag{18.99}$$

where

$$k = \sqrt{\frac{2\mu E}{\hbar^2}}; \quad k_1 = \sqrt{\frac{2\mu\,(E + V_0)}{\hbar^2}}. \tag{18.100}$$

[For $V_0 < 0$, k_1 is replaced by $k_2 = \sqrt{2\mu\,(E - V_0)\,/\hbar^2}$. Although k_2 is purely imaginary for $E < V_0$, $j_\ell(k_2 r)$ is still real.] Matching the radial wave function and its derivatives at $r = a$, I find

$$A_\ell j_\ell(x) + B_\ell n_\ell(x) = C_\ell j_\ell(x_1) \tag{18.101a}$$

$$A_\ell k j'_\ell(x) + B_\ell k n'_\ell(x) = C_\ell k_1 j'_\ell(x_1) \tag{18.101b}$$

where $j'_\ell(x)$ is a shorthand notation for $dj_\ell(y)/dy|_{y=x}$, $n'_\ell(x)$ is a shorthand notation for $dn_\ell(y)/dy|_{y=x}$, and

$$x = ka; \quad x_1 = k_1 a. \tag{18.102}$$

The partial wave phase shifts are given by Eq. (18.54c), namely

$$\tan\delta_\ell = -\frac{B_\ell}{A_\ell}. \tag{18.103}$$

Solving Eqs. (18.101), I find

$$\tan\delta_\ell = -\frac{B_\ell}{A_\ell} = \frac{xj_\ell(x_1)j'_\ell(x) - x_1 j_\ell(x)j'_\ell(x_1)}{xn'_\ell(x)j_\ell(x_1) - x_1 j'_\ell(x_1)n_\ell(x)}. \tag{18.104}$$

In effect I have solved the problem since all the phase shifts can be evaluated easily using a simple computer program. Once I have calculated the phase shifts from Eq. (18.104), I can construct

$$f_k(\theta) = \frac{1}{k}\sum_{\ell=0}^{\infty}(2\ell+1)e^{i\delta_\ell}\sin\delta_\ell P_\ell(\cos\theta); \tag{18.105a}$$

$$\sigma_k = \frac{4\pi}{k^2}\sum_{\ell=0}^{\infty}(2\ell+1)\sin^2\delta_\ell. \tag{18.105b}$$

The dimensionless variables that enter are

$$x = ka; \quad x_1 = \sqrt{x^2+\beta^2}; \quad \beta = \sqrt{\frac{2\mu V_0 a^2}{\hbar^2}}. \tag{18.106}$$

From your work on the eigenenergies of a particle in a spherical potential well, you will recognize that β is a measure of the number of bound states in the potential.

Low Energy - $x = ka \ll 1$

In this limit, only $\ell = 0$ contributes significantly and

$$\frac{d\sigma}{d\Omega} \approx \frac{\sin^2\delta_0}{k^2}; \tag{18.107a}$$

$$\sigma \approx 4\pi\frac{\sin^2\delta_0}{k^2}. \tag{18.107b}$$

For spherical barrier potentials, the dependence of the cross section on β is somewhat boring (see problems) and need not be discussed.

Spherical well potentials present a whole new story. There are values of β for which $\delta_0 = 0$ and S wave scattering is totally suppressed—this is known as the *Ramsauer-Townsend effect*. On the other hand, there are values of $\beta = (n+1/2)\pi$ for which bound states in the potential well occur near zero energy—the first such state occurs when $\beta = \pi/2$. For these values of β there is a *resonance* near $x = ka = 0$ and the wave function "bounces back and forth many times" as it is scattered. As a result the scattering cross section has a narrow, sharply peaked resonance as a function of β for fixed x.

These features are seen clearly in Figs. 18.17 and 18.18 where both the resonances and Ramsauer-Townsend effect can be seen. Note that this does not necessarily imply there is a resonance in the cross section as a function of *energy*

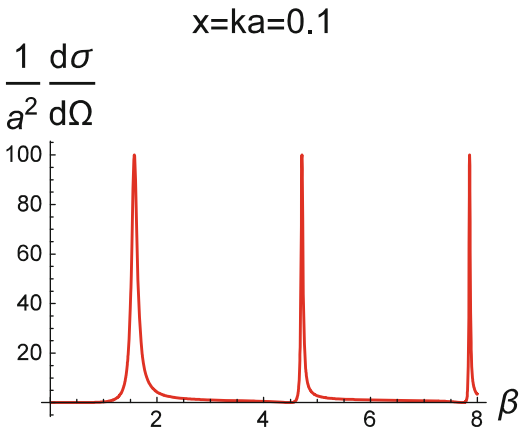

Fig. 18.17 Differential scattering cross section (in units of a^2) as a function of well strength parameter β

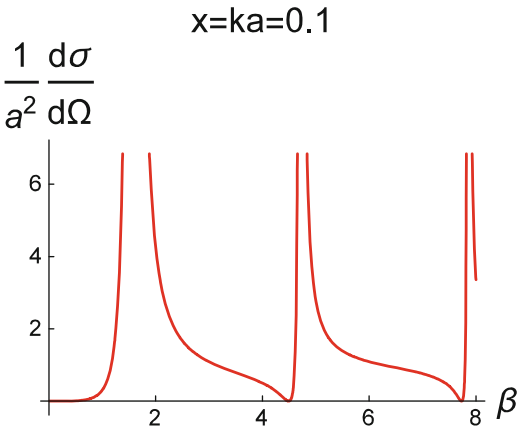

Fig. 18.18 Blow-up of Fig. 18.17 showing the Ramsauer-Townsend effect

for fixed β. The resonance effect at low energy is related to that associated with the perfect transmission for a one-dimensional square-well potential having width $2a$ [see Eq. (6.110) with a replaced by $2a$].

An expression for the differential cross section can be obtained without difficulty by substituting in the values of the spherical Bessel and Neumann functions and their derivatives for $\ell = 0$. Alternatively you can solve the radial equation directly for $\ell = 0$. Using either method, and setting $x_1 \approx \beta$ since $x \ll 1$, you will find

$$\tan \delta_0 = x \left(\frac{\tan \beta}{\beta} - 1 \right), \tag{18.108a}$$

$$\sin\delta_0 = \frac{x\left(\frac{\tan\beta}{\beta}-1\right)}{\sqrt{1+x^2\left(\frac{\tan\beta}{\beta}-1\right)^2}}, \tag{18.108b}$$

and

$$\frac{d\sigma}{d\Omega} \approx \frac{\sin^2\delta_0}{k^2} = \frac{a^2\left(\frac{\tan\beta}{\beta}-1\right)^2}{1+x^2\left(\frac{\tan\beta}{\beta}-1\right)^2}. \tag{18.109}$$

Note that, as a function of β, there are resonances whenever $\beta = (n+1/2)\pi$. At the resonance positions, $a^{-2}d\sigma/d\Omega = 1/x^2$ and the width $\Delta\beta$ of the resonances is of order x. There is a Ramsauer-Townsend effect whenever $\tan\beta/\beta = 1$.

Since $x \ll 1$, for all values of β except those corresponding to resonance,

$$\frac{d\sigma}{d\Omega} \approx a^2\left(\frac{\tan\beta}{\beta}-1\right)^2 = a_s^2 \tag{18.110}$$

where

$$a_s = -a\left(\frac{\tan\beta}{\beta}-1\right) = \lim_{k\to 0}\left(-\frac{1}{k}\tan\delta_0\right) \tag{18.111}$$

is referred to as the *scattering length*. Thus, low energy scattering can be characterized by a single parameter a_s, except in the region of a resonance (where a second parameter called the effective range r_{eff} is also needed). This is a very general result for any type of low energy scattering. In other words, the specific form of the potential is unimportant; the low energy cross section depends only on the scattering length which, in turn, depends on some *integral* property of the potential, such as the strength parameter β.

There is a simple geometric interpretation that can be given to the scattering length. Recall that the radial equation for $\ell = 0$ is simply

$$\begin{cases} \frac{d^2u_0(r)}{dr^2} + k_1^2 u_0(r) = 0 & r < a \\ \frac{d^2u_0(r)}{dr^2} + k^2 u_0(r) = 0 & r > a \end{cases}. \tag{18.112}$$

The general solution of these equations satisfying the boundary condition that $u_0(0) = 0$ is

$$\begin{cases} u_0(r) = A\sin(k_1 r) & r < a \\ u_0(r) = B\sin(kr+\delta_0) & r > a \end{cases}. \tag{18.113}$$

Matching the radial wave functions and their derivatives at $r = a$, and using the fact that $x = ka \ll 1$, I obtain the solution

$$u_0(r) \approx \begin{cases} A \sin(\beta r/a) & r < a \\ \frac{A \sin\beta}{x\cos\delta_0 + \sin\delta_0} \sin(xr/a + \delta_0) & r > a \end{cases}, \tag{18.114}$$

where δ_0 is determined from Eq. (18.108a). The value of β determines how many oscillations there are in $u_0(r)$ in the region $r < a$ [there are no oscillations for a *spherical barrier* potential since $\sin(\beta r/a) \to i \sinh(\beta r/a)$ which increases monotonically for $r < a$]. The slope of the radial wave function at $r = a$,

$$\left.\frac{du_0(r)}{dr}\right|_{r=a} = \frac{A\beta}{a}\cos(\beta), \tag{18.115}$$

is associated with the tangent to the function $u_0(r)$ at that point. I extend this tangent and look for the point r_s where it crosses the r-axis (see Fig. 18.19). I can calculate r_s using

$$u_0(a) - \left.\frac{du_0(r)}{dr}\right|_{r=a}(a - r_s) = u_0(r_s) = 0, \tag{18.116}$$

which has as solution

$$r_s = a\left(1 - \frac{\tan\beta}{\beta}\right) = -\frac{\tan(\delta_0)}{k} = a_s. \tag{18.117}$$

In other words, the scattering length is the radius at which the tangent to the radial wave function $u_0(r)$ at $r = a$ crosses the r-axis. For spherical well potentials with $\beta < \pi/2$, the slope is positive but always less than $u_0(a)/a$; consequently, $a_s < 0$. Since $a_s \neq 0$ there is no Ramsauer-Townsend when $\beta < \pi/2$. At the first resonance, $\beta = \pi/2$, $a_s = -\infty$ (the tangent is parallel to the r-axis), but for a value of β slightly larger than $\pi/2$ the wave function "turns over" and the scattering length becomes positive, mimicking the effects of a repulsive potential. This is how the scattering in a Bose condensate can appear to be repulsive, even if the actual potential is attractive. For still larger values of β, the scattering length decreases and eventually passes through $a_s = 0$, giving rise to the Ramsauer-Townsend effect, just before the next resonance. These features are illustrated in Fig. 18.19. [For spherical barrier potentials the radial wave function varies as $\sinh(\beta r/a)$ and the slope at $r = a$, $A\beta\cosh(\beta)/a$, is positive and always greater than $u_0(a)/a = A\tanh(\beta)/a$; consequently, $a_s > 0$.]

High Energy - $x = ka \gg 1$

When I consider scattering at high energies, a new range of phenomena can appear. I have already noted that the scattering is analogous to scattering by a dielectric sphere having index of refraction

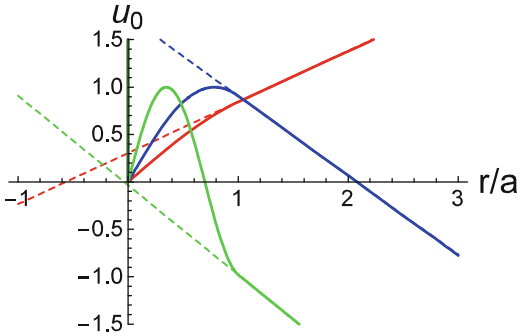

Fig. 18.19 Graphs of u_0 as a function of r/a for a spherical well potential with $A = 1, x = 0.1$ and $\beta = 1$ (red curve), 2 (blue curve), 4.5 (green curve). The dashed curves intersect the horizontal axis at a value corresponding to the scattering length. For $\beta = 1$, the scattering length is negative, for $\beta = 2$, the scattering length is positive, and for $\beta = 4.5$, the scattering length is zero (Ramsauer-Townsend effect)

$$n_{\text{eff}} = \sqrt{1 + \frac{V_0}{E}} = \sqrt{1 + \frac{\beta^2}{x^2}}. \tag{18.118}$$

Therefore, for $x = ka \gg 1$ and β of order unity, the index approaches unity and there is very little scattering. The more interesting regime is when x and β are comparable, so that n_{eff} is on the order or 1.4 or so. In that limit, one may see such effects as rainbow and glory scattering, although it may be necessary to go to values of x as large as 1000 to clearly see the rainbow effects.

I need to consider three ranges of angular momenta values to get a qualitative understanding of the scattering. First consider $\ell < ka$ which corresponds to impact parameters $b < a$ [see Fig. 18.20 with energy E_3]. This is analogous to the situation in optics where a ray enters the dielectric sphere and undergoes internal reflections in the sphere. Both rainbow and glory scattering occur. You can almost "see" the result. If a "particle" comes in, it is reflected and transmitted at $r = a$, reaches a point of closest approach r_0 and then is transmitted and reflected on its way out at $r = a$. The wave that exits the sphere is the "normal" refracted wave, but that wave is also reflected on the inner surface of the sphere and can emerge at some other direction and correspond to rainbow scattering for some incident impact parameter. Since an infinite number of reflections are possible, all scattering angles can occur and glory scattering occurs a well.

For $\ell > x_1 = \sqrt{x^2 + \beta^2}$, any penetration into the barrier is weak and there is very little scattering since $b \gg a$ [see Fig. 18.20 with energy E_1]. No tunneling into a classically allowed region is possible. However for $x_1 > \ell > x$, such tunneling is possible even though the impact parameter $b > a$ (this is a wave-like effect) [see Fig. 18.20 with energy E_2]. Most of the time the scattering is negligible, but if the

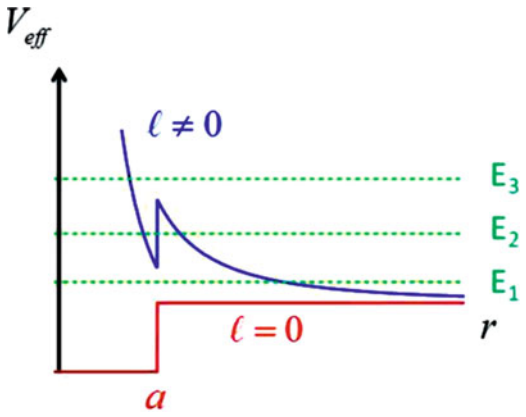

Fig. 18.20 Effective potential for a spherical well potential

incident energy corresponds to the energy of the quasi-bound states in the effective potential, there can be very narrow resonances in the scattering at these energies. Of course, the differential scattering cross section involves a sum over all values of ℓ, so all three types of effects are present at once.

The differential scattering cross section is shown in Figs. 18.21, 18.22, and 18.23, for $x = ka = \beta = 5, 20, 100$. There is a forward diffraction peak as in scattering by a hard sphere, but now there is evidence for glory scattering at $\theta = \pi$. Moreover, for this value of the effective index of refraction, $n_{\text{eff}} = \sqrt{2}$, the rainbow angle is predicted to be $\theta \approx 2.6\,\text{rad}$; the peak at this value in the $ka = 100$ graph, which sharpens with increasing ka, may be an indication that rainbow scattering is occurring. The oscillations in the graph correspond to interference effects arising from contributions from different ℓ to scattering at a given angle.

The classical differential cross section, given in Eq. (18.28) with $n = n_{\text{eff}} = \sqrt{1 + V_0/E}$, is also plotted in Figs. 18.21, 18.22 and 18.23 as the dashed curves. The classical cross section does not have a forward diffraction peak, but otherwise is in good agreement with the quantum distribution, averaged over oscillations, in the classically allowed region, which extends to $\theta_{\text{max}} = 2\cos^{-1}(1/n_{\text{eff}})$. For $n_{\text{eff}} = \sqrt{2}$, $\theta_{\text{max}} = \pi/2 = 1.57$.

For the case of scattering by a spherical barrier potential I can carry over the results of those for the spherical well potential by replacing V_0 with $-|V_0|$. In the limit that $E \ll |V_0|$, the results are similar to that for hard sphere scattering. For $E > |V_0|$, the net change from the attractive case is that the effective index is now $n_{\text{eff}} = \sqrt{1 - \frac{|V_0|}{E}}$ and the quantity β becomes pure imaginary. There is no longer any rainbow scattering and the interference effects that are present for scattering by a spherical well potential are diminished, since there are not as many impact

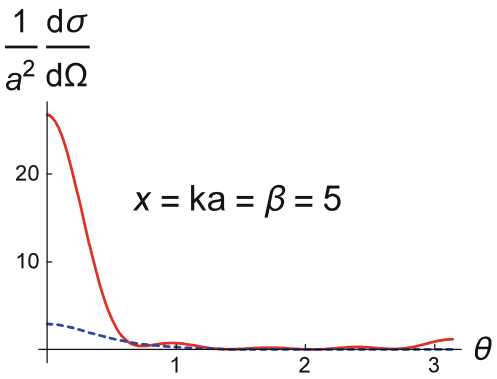

Fig. 18.21 Scattering by a spherical well potential showing the forward diffraction peak. The dashed, blue curve is the corresponding result for classical particle scattering, for which the diffraction peak is absent

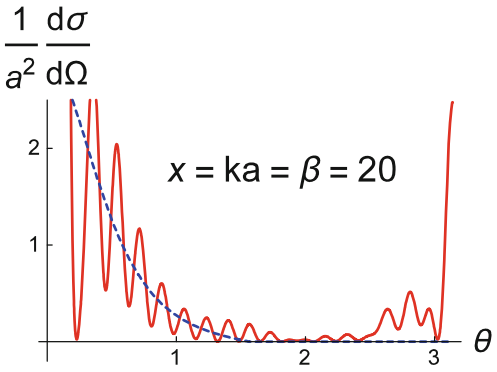

Fig. 18.22 Scattering by a spherical well potential showing the glory. The dashed, blue curve is the classical result

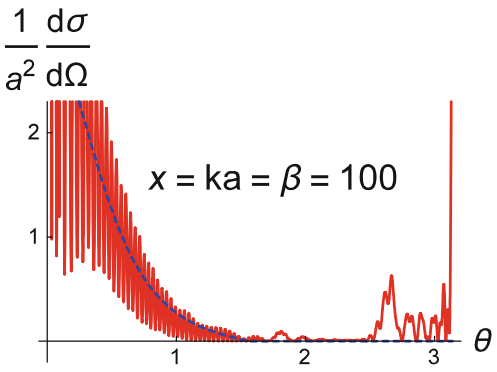

Fig. 18.23 Scattering by a spherical well potential showing the glory and a possible rainbow. The dashed, blue curve is the classical result

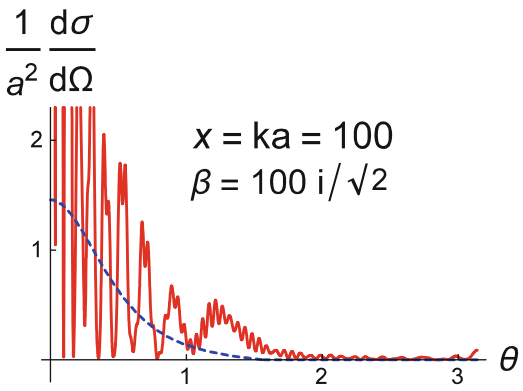

Fig. 18.24 Scattering by a spherical barrier potential. The dashed, blue curve is the classical result

parameters that give rise to the same scattering angle for repulsive scattering as there are for attractive scattering. In Fig. 18.24, where $x = 100$ and $\beta = 100i/\sqrt{2}$ ($n_{\text{eff}} = 1/\sqrt{2}$), you can see that there are fewer oscillations than in the corresponding case of scattering by a spherical well potential and that there is no rainbow, but there does appear to be a slight glory.

18.2.2 Born Approximation

For potentials requiring numerical solutions, the method of partial waves is especially useful in the low energy scattering limit, when only a few partial waves are needed. It would be good to have a result that is valid in the high energy limit, other than the WKB partial wave result. The *Born series* provides such a solution to this problem. The Born series is effectively a perturbative approach, valid when the scattering cross section can be expanded in a power series in the potential.

To derive the Born series, I start from the Schrödinger equation written in the form

$$\nabla^2\psi + k^2\psi = U(\mathbf{r})\psi, \tag{18.119}$$

where

$$U(\mathbf{r}) = \frac{2\mu}{\hbar^2}V(\mathbf{r}). \tag{18.120}$$

The idea is to treat the right-hand side as a perturbation. I look for a solution to this equation in the form

$$\psi_k(\mathbf{r}) = e^{i\mathbf{k}\cdot\mathbf{r}} - \frac{1}{4\pi}\int d\mathbf{r}' G(\mathbf{r}-\mathbf{r}')U(\mathbf{r}')\psi(\mathbf{r}'), \tag{18.121}$$

substitute it into Eq. (18.119) and find that, for this to be a solution, I must require that

$$\left(\nabla^2 + k^2\right) G(\mathbf{r}-\mathbf{r}') = -4\pi\delta(\mathbf{r}-\mathbf{r}'). \tag{18.122}$$

The quantity $G(\mathbf{r}-\mathbf{r}')$ is known as a *Green function*. It is not difficult to verify by direct substitution that

$$G(\mathbf{r}-\mathbf{r}') = \frac{e^{\pm ik|\mathbf{r}-\mathbf{r}'|}}{|\mathbf{r}-\mathbf{r}'|} \tag{18.123}$$

is a solution of Eq. (18.122). Which sign in the exponent to take depends on the physics. If the scattering is to correspond to *outgoing* spherical waves, the positive sign must be taken.

Thus, the formal solution for $\psi_k(\mathbf{r})$, obtained from Eqs. (18.121) and (18.123), is

$$\psi_k(\mathbf{r}) = e^{i\mathbf{k}\cdot\mathbf{r}} - \frac{1}{4\pi}\int d\mathbf{r}' \frac{e^{ik|\mathbf{r}-\mathbf{r}'|}}{|\mathbf{r}-\mathbf{r}'|}U(\mathbf{r}')\psi_k(\mathbf{r}'). \tag{18.124}$$

It looks like I haven't accomplished *anything* but to go from a differential to an integral equation. However, this is precisely the form that is useful for an iterative or perturbation series solution in powers of $U(\mathbf{r})$. In other words, to zeroth order in $U(\mathbf{r})$

$$\psi_k^{(0)}(\mathbf{r}) = e^{i\mathbf{k}\cdot\mathbf{r}} \tag{18.125}$$

and to first order

$$\psi_k^{(1)}(\mathbf{r}) = e^{i\mathbf{k}\cdot\mathbf{r}} - \frac{1}{4\pi}\int d\mathbf{r}' \frac{e^{ik|\mathbf{r}-\mathbf{r}'|}}{|\mathbf{r}-\mathbf{r}'|}U(\mathbf{r}')e^{i\mathbf{k}\cdot\mathbf{r}'}, \tag{18.126}$$

which is known as the *first Born approximation*. You can continue iterating the solution to obtain the Born series as a power series in the potential, but it is usually difficult to go beyond the first term. The first Born approximation is the most important result in high energy scattering.

To get the scattering amplitude, I must compare Eq. (18.126) in the limit $r \to \infty$ with Eq. (18.31). To do so, I take the z axis along $\mathbf{k}$, and expand

$$e^{ik|\mathbf{r}-\mathbf{r}'|} \approx e^{ikr(1-\hat{\mathbf{r}}\cdot\mathbf{r}')} = e^{ikr}e^{-i\mathbf{k}'\cdot\mathbf{r}'}, \tag{18.127}$$

where

$$\mathbf{k}' = k\mathbf{u}_r \tag{18.128}$$

gives the direction of scattering. In this manner, I find that as $r \to \infty$,

$$\psi_k^{(1)}(\mathbf{r}) \sim e^{ikz} - \frac{e^{ikr}}{4\pi r}\int d\mathbf{r}' e^{-i\mathbf{q}\cdot\mathbf{r}'} U(\mathbf{r}'), \tag{18.129}$$

where

$$\mathbf{q} = \mathbf{k}' - \mathbf{k}. \tag{18.130}$$

Comparing Eqs. (18.31) and (18.129), I obtain the scattering amplitude

$$f_k(\theta) = -\frac{1}{4\pi}\int d\mathbf{r} e^{-i\mathbf{q}\cdot\mathbf{r}} U(\mathbf{r}) = -\frac{\mu}{2\pi\hbar^2}\int d\mathbf{r} e^{-i\mathbf{q}\cdot\mathbf{r}} V(\mathbf{r}). \tag{18.131}$$

For spherically symmetric potentials, $V(\mathbf{r})$ is a function of r only. In this limit, to evaluate the integral, I take z along $\mathbf{q}$ such that

$$\mathbf{q}\cdot\mathbf{r} = qr\cos\theta, \tag{18.132}$$

enabling me to compute

$$\begin{aligned}\int d\mathbf{r} e^{-i\mathbf{q}\cdot\mathbf{r}} V(r) &= \int d\mathbf{r} e^{-iqr\cos\theta} V(r)\\ &= 2\pi\int_0^\infty r^2 dr\int_{-1}^1 d(\cos\theta) e^{-iqr\cos\theta} V(r)\\ &= \frac{4\pi}{q}\int_0^\infty dr \sin(qr)\, rV(r),\end{aligned} \tag{18.133}$$

such that

$$f_k(\theta) = -\frac{2\mu}{q\hbar^2}\int_0^\infty dr \sin(qr)\, rV(r). \tag{18.134}$$

The magnitude of $\mathbf{q}$ is given by

$$q = \left|\mathbf{k}' - \mathbf{k}\right| = k\left|\mathbf{u}_r - \mathbf{u}_z\right| = k\sqrt{2(1-\cos\theta)} = 2k\sin(\theta/2). \tag{18.135}$$

Roughly speaking, Eq. (18.134) is the Fourier sine transform of r times the potential. The hope is that the dependence of the Born cross section on q will reveal something about the nature of the potential giving rise to the scattering.

It is difficult to give a rigorous estimate of the corrections to the first Born approximation. Sometimes the Born approximation is used without justification since it is the only simple calculation that can be carried out. By looking at the second order term in the Born series and evaluating the terms in the integrand at $r = 0$, one can estimate that the first Born approximation is valid if

$$\left| \frac{\mu}{k\hbar^2} \int_0^\infty dr V(r) \left[e^{2ikr} - 1 \right] \right| \ll 1. \tag{18.136}$$

If there is some effective range a_0 to the potential and if the maximum of the potential is V_0, then the validity condition given by Eq. (18.136) reduces to

$$\mu V_0 a_0^2/\hbar^2 \ll 1 \text{ if } ka_0 \ll 1; \tag{18.137a}$$

$$\mu V_0 a_0^2/\left(ka_0\hbar^2\right) \ll 1 \text{ if } ka_0 \gg 1. \tag{18.137b}$$

Looking at Eq. (18.137b), you see that the first Born approximation is generally valid for high energy scattering, $ka_0 \gg 1$. It can be valid even for low energy scattering if $\beta^2 = 2\mu V_0 a_0^2/\hbar^2 \ll 1$; that is, for values of the strength β that are sufficiently small to insure that *no bound states could exist in the case of an attractive potential*. In fact, since condition (18.137a) is generally satisfied when condition (18.137b) holds, a sufficient condition for the Born series to converge is that $-|V(r)|$ is not strong enough to support a bound state (along with the additional requirements that both $\int_0^\infty dr\,|V(r)|\,r$ and $\int_0^\infty dr\,|V(r)|\,r^2$ are finite). Although conditions (18.137) are sufficient, they may not be *necessary* for validity of the first Born approximation.

Examples:

If

$$V(r) = V_0 e^{-r^2/a^2}, \tag{18.138}$$

then

$$\begin{aligned} f_k(\theta) = f(q) &= -\frac{2\mu V_0}{q\hbar^2} \int_0^\infty dr \sin(qr)\, r e^{-r^2/a^2} \\ &= -\frac{2\mu V_0}{q\hbar^2} \left[\frac{\sqrt{\pi}}{4} a^3 q e^{-a^2q^2/4} \right] = -\frac{\mu V_0 \sqrt{\pi} a^3 e^{-a^2q^2/4}}{2\hbar^2} \end{aligned} \tag{18.139}$$

and

$$\frac{d\sigma}{d\Omega} = |f_k(\theta)|^2 = \pi a^2 \left[\left(\frac{\mu V_0 a^2}{2\hbar^2} \right)^2 e^{-2k^2a^2 \sin^2(\theta/2)} \right], \tag{18.140}$$

where Eq. (18.135) was used. For $ka \gg 1$, the differential cross section exhibits a diffraction-like central peak with a maximum at $\theta = 0$, but, in contrast to the diffraction pattern of an opaque disk, there are no oscillations for larger values of θ. Note that, if $ka \ll 1$, $d\sigma/d\Omega$ is constant, as for any low energy S-wave scattering.

The first Born approximation is valid if condition (18.136) holds

$$\left| \frac{\mu V_0}{k\hbar^2} \int_0^\infty dr e^{-r^2/a^2} \left[e^{2ikr} - 1 \right] \right| \ll 1, \tag{18.141}$$

which can be rewritten as

$$\left| \frac{\beta^2}{2x} \int_0^\infty d\rho e^{-\rho^2} \left[e^{2ix\rho} - 1 \right] \right| \ll 1, \tag{18.142}$$

where $x = ka$. The integral can be evaluated in terms of known functions, but can also be done numerically. The inequality is satisfied for $\beta \ll 1$ if $x \leq 1$ and for $\beta^2 \ll x$ if $x \gg 1$.

As a second example, I take

$$V(r) = \begin{cases} -V_0 & r \leq a \\ 0 & r > a \end{cases}. \tag{18.143}$$

For this potential

$$\begin{aligned} f_k(\theta) = f(q) &= \frac{2\mu V_0}{q\hbar^2} \int_0^a dr \sin(qr)\, r \\ &= \frac{2\mu V_0}{q\hbar^2} \left[\frac{\sin(aq) - aq\cos(aq)}{q^2} \right] \end{aligned} \tag{18.144}$$

and

$$\frac{d\sigma}{d\Omega} = |f(q)|^2 = a^2\beta^4 \left[\frac{\sin(aq) - aq\cos(aq)}{q^3 a^3} \right]^2, \tag{18.145}$$

where

$$\beta = \sqrt{\frac{2\mu V_0 a^2}{\hbar^2}} \tag{18.146}$$

is a measure of the number of bound states supported by the potential. Recall that $q = 2k\sin(\theta/2)$.

If $ka \ll 1$, then

$$\frac{d\sigma}{d\Omega} \sim \frac{\beta^4 a^2}{9} \tag{18.147}$$

and the scattering is isotropic. This low energy result agrees with Eq. (18.110) obtained using the method of partial phases, provided $\beta \ll 1$ [in that limit, $(\tan\beta/\beta - 1)^2 \sim \beta^4/9$].

Next consider the limit that $qa \gg 1$, that is, high energy scattering outside the diffraction cone defined by $\theta_d \approx 1/ka$. In this case,

$$f(q) \sim -\beta^2 a \frac{\cos(aq)}{q^2 a^2} \tag{18.148}$$

and

$$\frac{d\sigma}{d\Omega} \sim \beta^4 a^2 \frac{\cos^2(aq)}{q^4 a^4}. \tag{18.149}$$

Inside the diffraction cone, that is, for $\theta_d \ll 1/ka$, the result is still given by Eq. (18.147). The overall pattern is similar to that for Fraunhofer diffraction of optical radiation by a circular aperture.

According to conditions (18.136), the first Born approximation should be valid if

$$\left|\frac{\mu V_0}{k\hbar^2}\int_0^a dr\left[e^{2ikr} - 1\right]\right| = \frac{\beta^2}{2x}\left|\left[\frac{e^{2ix} - 1}{2ix} - 1\right]\right| \ll 1, \tag{18.150}$$

where $x = ka$. Thus the first Born approximation is valid for $\beta^2 \ll 1$ if $x \ll 1$ and for $\beta^2/x \ll 1$ if $x \gg 1$. However these are sufficient, but not necessary conditions. By comparing the exact solution given by Eqs. (18.104)–(18.105), you can show that if $\beta/x = \sqrt{V_0/E} \ll 1$, then the first Born approximation is valid for all θ. This limit corresponds to scattering by a sphere whose effective index of refraction is approximately equal to unity.

The total cross section is given by

$$\begin{aligned}\sigma_k &= 2\pi\int_0^\pi |f(q)|^2 \sin\theta d\theta \\ &= \frac{2\pi a^2\beta^4}{k^2a^2}\int_0^{2ka} dy\frac{[\sin y - y\cos y]^2}{y^5} \\ &= \pi\beta^4 a^2\left[\frac{32x^4 - 8x^2 - 1 + 4x\sin(4x) + \cos(4x)}{64x^6}\right],\end{aligned} \tag{18.151}$$

where Eq. (18.145) was used along with the substitutions $y = qa = 2ka\sin(\theta/2) = 2x\sin(\theta/2)$ and $\sin\theta = 2\sin(\theta/2)\cos(\theta/2)$.

Note that the Born approximation can fail even in the limit $\hbar \sim 0$ ($ka \sim \infty$), owing to the sharp boundary of the spherical potential well. That is, in the limit $ka = x \gg 1$,

$$\sigma \sim \frac{\pi a^2 \beta^4}{2x^2} = \frac{\pi a^2 \beta^2}{2} \left(\frac{\beta}{x}\right)^2, \tag{18.152}$$

which is a good approximation to the total cross section when $\beta/x = \sqrt{V_0/E} \ll 1$. However, if $\beta = x \gg 1$, this result is not valid since it gives $\sigma \sim \pi a^2 \beta^2/2$ whereas the correct cross section, calculated from Eqs. (18.105) and (18.104), is of order $2\pi a^2$.

18.3 Summary

I have given a rather detailed discussion of elementary quantum scattering theory, trying to emphasize the underlying physics. To facilitate the discussion, I reviewed aspects of classical scattering of particles and electromagnetic radiation, since many features encountered in classical scattering, such as rainbows and glories, resurface in quantum scattering theory. There are two different methods that can be used to solve the quantum scattering problem. The method of partial waves is especially useful for low energy scattering while the Born approximation is basically a high energy, perturbative approach. Scattering by various potentials was considered and different types of resonance phenomena were explored, as were diffractive effects associated with sharp changes in the scattering potential.

18.4 Appendix A: Free Particle Solution in Spherical Coordinates

For a free particle, we know that the (unnormalized) eigenfunctions are simply

$$\psi_k(\mathbf{r}) = e^{i\mathbf{k}\cdot\mathbf{r}}, \tag{18.153}$$

where $k^2 = 2\mu E/\hbar^2$. Why should we go the trouble of solving this in spherical coordinates when there is no natural origin to the problem? The reason for this is that, although the particle is not free in the scattering problem, the functional form of the eigenfunctions for the region $r > r_{\max}$ is the same as that of a free particle, provided the potential vanishes for $r > r_{\max}$.

To solve the free particle problem in spherical coordinates, I recall, that for any spherically symmetric potential, the eigenfunctions have the form

$$\psi_{k\ell m}(\mathbf{r}) = R_\ell(r) Y_\ell^m(\theta, \phi), \tag{18.154}$$

where the $Y_\ell^m(\theta,\phi)$s are spherical harmonics and $R_\ell(r) = u_\ell(r)/r$ and $u_\ell(r)$ satisfy the radial equations

$$\frac{1}{r^2}\frac{d}{dr}\left(r^2\frac{dR_\ell}{dr}\right) + \left[k^2 - \frac{2\mu V(r)}{\hbar^2} - \frac{\ell\,(\ell+1)}{r^2}\right]R_\ell = 0; \tag{18.155a}$$

$$\frac{d^2u_\ell}{dr^2} + \left[k^2 - \frac{2\mu V(r)}{\hbar^2} - \frac{\ell\,(\ell+1)}{r^2}\right]u_\ell = 0. \tag{18.155b}$$

For $V(r) = 0$, the equations are

$$\frac{d}{dr}\left(r^2\frac{dR_\ell}{dr}\right) + k^2r^2R_\ell - \ell\,(\ell+1)\,R_\ell = 0; \tag{18.156a}$$

$$\frac{d^2u_\ell}{dr^2} + k^2u_\ell - \frac{\ell\,(\ell+1)}{r^2}u_\ell = 0, \tag{18.156b}$$

having linearly independent solutions that are spherical Bessel and Neumann functions,

$$R_\ell^{(1)}(kr) = j_\ell(x) = \sqrt{\frac{\pi}{2x}}J_{\ell+1/2}(x); \tag{18.157a}$$

$$R_\ell^{(2)}(kr) = n_\ell(x) = \sqrt{\frac{\pi}{2x}}N_{\ell+1/2}(x), \tag{18.157b}$$

where $J_\ell(x)$ and $N_\ell(x)$ are ordinary Bessel and Neumann functions and $x = kr$. For the free particle, the Neumann function solutions must be rejected because they are not regular at the origin.

As a consequence, the free particle eigenfunction $e^{i\mathbf{k}\cdot\mathbf{r}}$ can be expanded in terms of spherical harmonics and spherical Bessel functions as

$$\psi_k(\mathbf{r}) = e^{i\mathbf{k}\cdot\mathbf{r}} = \sum_{\ell=0}^{\infty}\sum_{m=-\ell}^{\ell} A_{\ell m}j_\ell(kr)Y_\ell^m(\theta,\phi). \tag{18.158}$$

It is not trivial to find the expansion coefficients $A_{\ell m}$ directly from Eq. (18.158), but it can be shown that[3]

$$A_{\ell m} = 4\pi i^\ell\left[Y_\ell^m(\theta_k,\phi_k)\right]^*, \tag{18.159}$$

[3] Actually, Eq. (18.159) can be derived from Eq. (18.160) using the addition theorem for spherical harmonics. For a derivation of the addition theorem, see George Arfken, *Mathematical Methods for Physicists*, Third Edition (Academic Press, San Diego, 1985).

where (θ_k, ϕ_k) are the polar and azimuthal angles of the vector $\mathbf{k}$. If the z axis is taken along $\mathbf{k}$, then $\theta_k = 0$ and Eq. (18.158) reduces to

$$e^{ikz} = e^{ikr\cos\theta} = \sum_{\ell=0}^{\infty} i^\ell (2\ell+1) j_\ell(kr) P_\ell(\cos\theta), \tag{18.160}$$

the result I needed to obtain the scattering amplitude using the method of partial waves.

I can give a simple derivation of Eq. (18.160). In Eq. (18.158) with the z axis taken along $\mathbf{k}$, the left-hand side is independent of ϕ so I can set $\phi = 0$ in the right-hand side. Then the spherical harmonics reduce to Legendre polynomials and the sum over m can be carried out, enabling me to expand

$$e^{ikz} = e^{ikr\cos\theta} = \sum_{\ell'=0}^{\infty} B_{\ell'} j_{\ell'}(kr) P_{\ell'}(\cos\theta), \tag{18.161}$$

where the $B_{\ell'}$s are some new expansion coefficients. I multiply by $P_\ell(\cos\theta)$ and integrate over $\cos\theta$ using the orthogonality of the Legendre polynomials to obtain

$$B_\ell j_\ell(kr) = \frac{2\ell+1}{2} \int_{-1}^{1} dx e^{ikrx} P_\ell(x) dx, \tag{18.162}$$

where $x = \cos\theta$. I now take the limit that $r \to \infty$ on both sides. On the right-hand side I can integrate by parts using $u = P_\ell(x)$ and $dv = e^{ikrx}$ and on the left-hand side I use Eq. (18.48) to arrive at

$$B_\ell \frac{\sin\left(kr - \frac{\ell\pi}{2}\right)}{kr} = \frac{2\ell+1}{2} \left[\frac{P_\ell(1)e^{ikr} - P_\ell(-1)e^{ikr}}{ikr} \right]. \tag{18.163}$$

I have neglected the integral term in the integration by parts since it vanishes in the limit $r \to \infty$ (you can see this by carrying out additional integration by parts on the integral term). Since $P_\ell(1) = 1$ and $P_\ell(-1) = (-1)^\ell$, it follows from Eq. (18.163) that

$$\begin{aligned} &B_\ell \frac{e^{ikr}e^{-i\ell\pi/2} - e^{-ikr}e^{i\ell\pi/2}}{2ikr} = \frac{2\ell+1}{2} \left[\frac{e^{ikr} - (-1)^\ell e^{-ikr}}{ikr} \right]; \\ &B_\ell e^{-i\ell\pi/2} \left(e^{ikr} - e^{-ikr}(-1)^\ell \right) = (2\ell+1) \left(e^{ikr} - (-1)^\ell e^{-ikr} \right); \\ &B_\ell = e^{i\ell\pi/2} (2\ell+1) = i^\ell (2\ell+1), \end{aligned} \tag{18.164}$$

and the proof is complete.

18.5 Appendix B: Hard Sphere Scattering when $ka \gg 1$

In this Appendix, I give some of the mathematical details for hard sphere scattering in the limit that $ka \gg 1$. The maximum value of ℓ that contributes to the sum over partial waves in Eq. (18.62) is approximately equal to ka. To apply asymptotic methods, I break the scattering into two regions, $\theta \ll (ka)^{-1/3}$ and $\theta \gg (ka)^{-1/3}$ in all cases I assume that $ka \gg 1$.

If $\theta \ll (ka)^{-1/3}$ and $\ell \lesssim ka$,

$$P_\ell(\cos\theta) \sim J_0\left[(\ell + 1/2)\,\theta\right], \tag{18.165}$$

where $J_0\left[(\ell + 1/2)\,\theta\right]$ is a normal Bessel function, leading to a scattering amplitude [Eq. (18.62)]

$$f_k(\theta) \approx \frac{1}{2ik}\sum_{\ell=0}^{\infty}(2\ell+1)\left(e^{2i\delta_\ell}-1\right)J_0\left[(\ell+1/2)\,\theta\right]. \tag{18.166}$$

The δ_ℓ are determined from Eq. (18.89). The function $e^{2i\delta_\ell}$ oscillates rapidly for $\ell < ka$ and goes to unity for $\ell > ka$, allowing me to write

$$f_k(\theta) \approx \frac{-1}{2ik}\sum_{\ell=0}^{ka}(2\ell+1)J_0\left[(\ell+1/2)\,\theta\right]. \tag{18.167}$$

I can set $z = \ell + 1/2$ and replace the sum by the integral to arrive at

$$f_k(\theta) \approx \frac{-1}{ik}\int_0^{ka} dz J_0\left[z\theta\right] z = \frac{ia}{\theta}J_1\left[ka\theta\right], \tag{18.168}$$

such that

$$\frac{d\sigma}{d\Omega} = |f_k(\theta)|^2 \approx \frac{a^2}{4}\left[\frac{2J_1\left[ka\theta\right]}{ka\theta}\right]^2 k^2a^2. \tag{18.169}$$

Equation (18.169) is valid for $0 \le \theta \ll (ka)^{-1/3}$, when $ka \gg 1$. The first minimum in the differential cross section occurs at $\theta \approx 3.83/ka < (ka)^{-1/3}$. As such, Eq. (18.169) correctly describes the forward diffraction peak associated with hard sphere scattering. Since $J_1(z) \sim z/2$ as $z \to 0$, the diffraction peak has an amplitude

$$\frac{d\sigma}{d\Omega}(\theta = 0) \approx \frac{a^2}{4}(ka)^2. \tag{18.170}$$

The contribution to the *total* cross section from the diffractive component can be obtained by assuming that most of the contributions come from small angles $\theta \lesssim 1/ka \ll (ka)^{-1/3}$. This allows me to replace $\sin\theta$ by θ and to replace the upper integration limit $(ka)^{-1/3}$ by ∞; that is,

$$\begin{aligned}\sigma_{\text{diff}} &= 2\pi\frac{k^2a^4}{4}\int_0^{(ka)^{-1/3}}\left[\frac{2J_1\left[ka\theta\right]}{ka\theta}\right]^2\sin\theta d\theta \\ &\approx 2\pi\frac{k^2a^4}{4}\int_0^{\infty}\left[\frac{2J_1\left[ka\theta\right]}{ka\theta}\right]^2\theta d\theta \\ &= 2\pi a^2\int_0^{\infty}\left[\frac{J_1(z)}{z}\right]^2 z dz = 2\pi a^2\left(\frac{1}{2}\right) = \pi a^2. \end{aligned} \tag{18.171}$$

To obtain the differential cross section outside the diffraction cone, that is, for $\theta \gg (ka)^{-1/3}$, I can approximate

$$P_\ell(\cos\theta) \sim \sqrt{\frac{1}{\pi\ell\sin\theta}}\cos\left[(\ell+1/2)\,\theta - \frac{\pi}{4}\right], \tag{18.172}$$

such that

$$f_k(\theta) \approx \frac{1}{2ik}\sum_{\ell=0}^{\infty}(2\ell+1)\left(e^{2i\delta_\ell}-1\right)\sqrt{\frac{1}{\pi\ell\sin\theta}}\cos\left[(\ell+1/2)\,\theta - \frac{\pi}{4}\right]. \tag{18.173}$$

Equation (18.172) is valid only for $\ell \gg 1$, but large values of ℓ provide the major contribution to the sum given in Eq. (18.173). The sum can be replaced by an integral and the method of stationary phase can be used to evaluate the integral. That is, after converting to an integral, for a given θ, there is a major contribution to the integral from the angular momentum (impact parameter) giving rise to the scattering at this angle; moreover, this impact parameter corresponds to the *classical* impact parameter giving rise to the scattering at this angle. This is a general result for high-energy scattering for any potential. Explicitly for the hard sphere potential, one finds

$$f_k(\theta) \approx \frac{a}{2}e^{i\alpha}, \tag{18.174}$$

where α is some phase that can be calculated using a WKB type approximation. Thus, *outside* the diffraction cone,

$$\frac{d\sigma}{d\Omega} = |f_k(\theta)|^2 \approx \frac{a^2}{4}, \tag{18.175}$$

the classical result.

The total cross section can be obtained directly from Eq. (18.168) as

$$\sigma = \frac{4\pi}{k}\,\mathrm{Im} f_k(0) = \frac{4\pi}{k}\frac{ka^2}{2} = 2\pi a^2. \tag{18.176}$$

The diffractive and classical scattering each contribute πa^2 to the total cross section.

18.6 Problems

1. Explain why specifying the impact parameter and the energy is equivalent to specifying the angular momentum and the energy in classical scattering by a spherically symmetric potential. Under what conditions can there be rainbow-like and glory scattering of classical particles? Why is the total cross section for classical scattering infinite for a potential having infinite range?

2. This problem refers to classical scattering.

(a) For the potential

$$V(r) = \begin{cases} 0, & r \geq a \\ \infty, & r < a \end{cases},$$

find the angular momentum for which the scattering angle goes to zero.

(b) For the potential

$$V(r) = -V_0 e^{-r^2/a^2},$$

where V_0 is positive, plot the effective potential as a function of r/a when

$$\frac{L^2}{2\mu a^2} = \frac{V_0}{3} = 100$$

in some appropriate energy units. For a particle of mass μ having energy $E > 0$, show that both bound and free orbits are possible. Indicate on the graph the energy for which orbiting can occur.

3. Outline the procedures that are used for solving a scattering problem using the method of partial waves and using the Born approximation. In general, when is each method most useful? Are there cases where only the $\ell = 0$ partial wave contributes, yet the first Born approximation gives a result that agrees with $\ell = 0$ scattering? Explain. Why can't the Born approximation give a good result for hard sphere scattering?

4–6. Consider the hard sphere potential,

$$V(r) = \begin{cases} 0 & r \geq a; \\ \infty & r < a \end{cases}.$$

Numerically obtain the *total* cross section for $x = ka = 0.1, 10, 100, 500$ and compare it with πa^2. You need only go from $\ell = 0$ to $\ell = ka + 25$ in evaluating the sum over partial waves in each case (why?). Interpret your result.

For $ka = 75$, numerically calculate and plot the differential scattering cross section for $\theta < 0.25$ and in the range $\pi/4 < \theta < \pi$. Interpret your results.

Plot $\cos(2\delta_\ell)$ as a function of ℓ for $ka = 50$ to illustrate that, for $ka \gg 1$, $\cos(2\delta_\ell)$ oscillates rapidly for $\ell < ka$ and is approximately equal to unity for $\ell > ka$. Use this result to show that the total cross section for $ka \gg 1$ is equal to $2\pi a^2$.

7–8. (a) In scattering of light rays by a sphere having index of refraction $n > 1$ and radius a, you can show using simple geometric optics (you are not asked to do this), that the scattering angle Θ_N after N internal reflections is given by Eq. (18.29), where b is the impact parameter of the incident light ray. Plot Θ_1 as a function of b/a, which mirrors classical scattering by a spherical well potential with $V_0/E = n^2 - 1$. Find the maximum value of $|\Theta_1|$. Also show that a primary rainbow ($N = 2$) exists for $n = \sqrt{2}$ and find the rainbow angle. Find the rainbow angle for $n = 4/3$ (water) and translate this result into an angle from which the rainbow is seen from Earth. For $n = \sqrt{2}$ show that contributions to glory scattering are possible, but only for $N \geq 4$.

(b) In the case of scattering by a sphere whose index of refraction relative to its surroundings is less than unity, Θ_N is given by Eq. (18.30). In this case, show that for $n = 1/\sqrt{2}$ that there is no rainbow scattering but contributions to glories are still possible for $N \geq 3$.

9–11. Now look at the quantum problem of scattering of a particle having mass μ by the spherical well potential,

$$V(r) = \begin{cases} -V_0 & r \leq a \\ 0 & r > a \end{cases},$$

with $V_0 > 0$. The scattering is analogous to scattering of electromagnetic radiation by a dielectric sphere having relative index of refraction

$$n_{\text{eff}} = \sqrt{1 + \frac{V_0}{E}}.$$

Take $V_0/E = 1$ and plot the differential cross section as a function of θ for $ka = 15$. Identify the structures in the cross section.

Next repeat the calculation for scattering by the spherical barrier potential

$$V(r) = \begin{cases} V_0 & r \le a \\ 0 & r > a \end{cases},$$

with $V_0/E = 1/2$. In this case, the scattering is analogous to the scattering of electromagnetic radiation by a bubble in a dielectric medium, when the index of refraction of the bubble relative to that of its surrounding medium is given by

$$n_{\text{eff}} = \sqrt{1 - \frac{V_0}{E}}.$$

Why does the qualitative structure of the differential cross sections differ?

In this problem you must sum the contributions from the phase shifts numerically. Do you see rainbow and glories in each case?

12. Derive Eq. (18.108a). Show that, for low energy scattering by a spherical barrier potential, the differential scattering cross section does not exhibit any of the resonant structures found for scattering by a spherical well potential.

13. Derive Eq. (18.114) and the corresponding result for scattering by a spherical barrier potential. Prove that the scattering length is always positive for scattering by a spherical barrier potential.

14. Prove that $G(\mathbf{r}) = e^{ikr}/r$ is a solution of the equation

$$\left(\nabla^2 + k^2\right) G(\mathbf{r}) = -4\pi\delta(\mathbf{r}).$$

You can use the fact that $\nabla^2(1/r) = -4\pi\delta(\mathbf{r})$. Hint: You can also use the fact that, for any two functions f and g,

$$\nabla^2(fg) = \boldsymbol{\nabla}\cdot\boldsymbol{\nabla}(fg) = \boldsymbol{\nabla}\cdot(f\boldsymbol{\nabla}g + g\boldsymbol{\nabla}f) = f\nabla^2 g + g\nabla^2 f + 2\boldsymbol{\nabla}f\cdot\boldsymbol{\nabla}g.$$

15. Calculate the differential scattering cross section in first Born approximation for a potential $V(r) = V_0\text{sech}(r/a)$. Plot your results as a function of θ for $\beta = \left(2\mu V_0/\hbar^2\right)^{1/2} a = 0.5$ and $x = ka = \left(2\mu E/\hbar^2\right)^{1/2} a = 2$. In general, when would you expect the Born approximation to be a good approximation for this potential?

16–17. Consider scattering by the spherical well potential,

$$V(r) = \begin{cases} -V_0 < 0 & r \le a \\ 0 & r > a \end{cases}.$$

Using the validity condition (18.136), show that the Born approximation is valid provided $\beta^2/x \ll 1$, when $x = ka \gg 1$.

Compare the exact solution [obtained using Eqs. (18.104) and (18.105a)] and the Born approximation result [Eq. (18.145)] for the differential cross section for $x = 10$

and $\beta = 1, x = 10$ and $\beta = 2$, and $x = 10$ and $\beta = 6$. Do you think the condition $\beta^2/x \ll 1$ is necessary for the validity of the Born approximation?

18. The total cross section for scattering by a spherical well potential in Born approximation is given by Eq. (18.151). You can try to reproduce this result, but it is not part of the problem. Find σ in the limit that $ka \ll 1$ and $ka \gg 1$. For $ka = 0.1, 1, 30$ compare the total cross section with that calculated "exactly" (that is, summing the partial waves) using the method of partial waves. In each case take a value of $\beta \ll ka$, $\beta = ka$, and $\beta \gg ka$. Under what conditions is the Born approximation valid?

19–20. Return to Problem 18.9–11 and plot two graphs of the total cross section (in units of πa^2) for $\beta = 10$ as a function of $x = ka$. In one graph take $0 \leq x \leq 20$ and in the second graph, take $20 \leq x \leq 100$. Show that there are resonances in the total cross section. The positions of the resonances should coincide with the energies of the quasibound states of the effective potential. To check this in a very *rough* manner, calculate the energies of the quasibound states for $\ell \leq 15$ using the WKB approximation,

$$\int_{r_1}^{r_2} k(r)dr = (n + 1/2)\,\pi,$$

where

$$k(r)a = \sqrt{x^2 + \beta^2 - \frac{\ell\,(\ell + 1)}{r^2/a^2}},$$

and r_1 and r_2 are the classical turning points of the classical bound states of the effective potential for energy $E > 0$ (the WKB approximation cannot be expected to provide accurate positions of the resonances since there is at most one bound state for each value of ℓ). For $x \gg 1$, compare your result with that of the Born approximation, $\sigma = \pi\beta^4/2x^2$. If you take larger values of β, there will be more quasibound states since the depth of the well in the effective potential and the number of quasibound states grows with increasing β.